University of New Hampshire
University of New Hampshire Scholars' Repository

Master's Theses and Capstones   Student Scholarship

Fall 2009

Extrapolating hyperspectral anthocyanin indices to multispectral satellite sensors---applications to fall foliage in New England

Erica Lindgren
University of New Hampshire, Durham

Follow this and additional works at: https://scholars.unh.edu/thesis

EXTRAPOLATING HYPERSPECTRAL ANTHOCYANIN INDICES TO

MULTISPECTRAL SATELLITE SENSORS—APPLICATIONS TO FALL FOLIAGE

IN NEW ENGLAND

BY
ERICA LINDGREN
BA, University of New Hampshire, 2005

THESIS

Submitted to the University of New Hampshire
In Partial Fulfillment of
The Requirements for the Degree of

Master of Science
in
Natural Resources

September, 2009

UMI Number: 1472071

INFORMATION TO USERS

The quality of this reproduction is dependent upon the quality of the copy
submitted.   Broken or indistinct print, colored or poor quality illustrations
and photographs, print bleed-through, substandard margins, and improper
alignment can adversely affect reproduction.
In the unlikely event that the author did not send a complete manuscript
and there are missing pages, these will be noted.   Also, if unauthorized
copyright material had to be removed, a note will indicate the deletion.
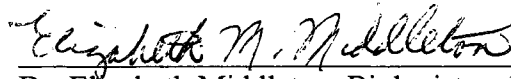
UMI®

This thesis has been examined and approved.

_____

Thesis Director, Dr. Barrett Rock,
Professor of Natural Resources and Earth, Oceans, and Space

_____

Dr. Elizabeth Middleton, Biologist and Remote Sensing Specialist,
NASA Goddard Space Flight Center

_____

Dr. John Aber, Professor of Natural Resources

_____8/13/09_____

Date

ACKNOWLEDGMENTS

TABLE OF CONTENTS

LIST OF TABLES
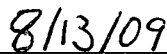
ABSTRACT

EXTRAPOLATING HYPERSPECTRAL ANTHOCYANIN INDICES TO MULTISPECTRAL SATELLITE SENSORS—APPLICATIONS TO FALL FOLIAGE IN NEW ENGLAND

by

Erica Lindgren

University of New Hampshire, September, 2009

Anthocyanin, thought to be a universal indicator of plant stress, is a red pigment found in many plant species and can seen in New England autumns. Detecting its presence is useful for ecosystem analysis and monitoring changes during autumn senescence. Currently fall foliage is subjectively measured; creation of a satellite-based anthocyanin index will provide an objective measurement and enhance understanding of the distribution of plant stress and senescence over large areas. Anthocyanin indices were tested hyperspectrally in a laboratory setting, then indices were simulated for Hyperion, MERIS, MODIS, and Landsat TM/ETM+ to see which most accurately represents changes in anthocyanin concentration, and finally indices were applied to actual imagery. Results of this study found that $(1/R564)-(1/R697)$ was the best approximation for anthocyanin; the red:green ratio was the best overall estimator of anthocyanin using simulated satellite bands; and real imagery from MODIS and MERIS satellite sensors can detect a fall foliage signal.

CHAPTER 1

LITERATURE REVIEW

Climate change is occurring due to rising greenhouse gases (ghg) (IPCC 2007). These

increasing ghg concentrations can change temperatures—which affect precipitation,

winds, and many other climatic variables (IPCC 2007). Changes in climate are important

because ecosystems are often defined by their relationship to temperature and

precipitation (Aber and Melillo 2001). Foliar color expression in the fall is thought to be

best when a tree is healthy, experiences reduced day length accompanied by a large daily

temperature gradient, is not subject to high winds, and when the weather is sunny with

few cloudy days (Clatterbuck 1999, Chaney 2005, Bardon 2007, Coder 2007). Changes

in temperature will affect the suitable habitat for trees which contribute to fall foliage, the

length of seasons, the severity of winds, the distribution of rainfall, and the population

distribution of pests and diseases—all of which will affect fall color expression (Menzel

and Fabian 1999, Inouye 2000, Dale *et al.* 2001, Rosenzweig *et al.* 2001, Walther *et al.*

2002). Data from the International Phenological Gardens have already shown in a 30-

year study, based on leaf color change, that foliage change is now delayed 4.8 days on

average in the northern hemisphere(Menzel and Fabian 1999).

Changes in the character of fall foliage are important as New England's fall foliage attracts millions of visitors each year, contributing to local tourism as well as the cultural identity of the region. The New Hampshire Division of Travel and Tourism Development (Tourism 2007) calls the fall "our busiest time of the year." State offices claim that foliage visitors comprise 20-25% of annual tourists in Vermont and Maine (New England Regional Assessment Group 2001). For example, in 2006, New Hampshire hosted about 7.75 million fall tourists who supported over a billion dollars in direct spending (Development 2007). The reaction of the northern hardwoods to the current climate supports a large tourism industry. If the climate were to change and affect fall foliage, it is likely that the tourism would respond correspondingly. Most methods for determining fall color intensity and timing changes are based on personal observations or previous perceived trends (Vermont Vacation 2009). While this information is useful it is extremely subjective. A more objective measurement method based on satellite data would be beneficial, both from the standpoint of predicting specific fall color displays and for comparing long-term trends in foliar color displays over the past several decades.

Plant pigments react to environmental stresses, such as those induced by climate change. Detecting and quantifying pigment content can greatly increase our knowledge about a plant's physiology and health as it reacts to these stresses. Although chlorophyll is the main photosynthetic pigment in plants, other pigments can absorb light, such as carotenoids, which absorb strongly in the blue region of the electromagnetic spectrum and have antioxidant properties. Anthocyanin is a pigment that is not involved in

photosynthesis but absorbs in the green region of the visible spectrum. Its synthesis has been implicated in everything from photoinhibition, UV protection, drought resistance, cold hardiness, antioxidation, herbivory defense, to certain types of nutrient deficiency (Chalker-Scott 1999, Close and Beadle 2003).

While the most accurate way to measure pigment concentrations is through destructive analysis, a large body of research has explored the development of non-destructive assessment methods through the use of remote sensing tools. Reflectance spectroscopy has been used for estimation of chlorophyll and accessory pigment concentrations (Rock *et al.* 1988, Blackburn 2007). Absorption features have been characterized for several pigments and derived spectral indices have been created to eliminate overlapping absorptions between varying pigments (Merzlyak *et al.* 1999, Gitelson and Merzlyak 2004). Researchers have developed hyperspectral indices for anthocyanin using a two or three band ratio. A band within 550-570nm accounts for anthocyanin absorbance in the green while a band within 700-710nm estimates chlorophyll's reflectance and is used to subtract it's effects in the green region; some indices also include a band in the near IR (750-800nm) to account for leaf structure (Merzlyak *et al.* 1999, Gitelson *et al.* 2001a, Sims and Gamon 2002, Gitelson *et al.* 2006).

Extrapolation of ground-based anthocyanin indices to satellite systems has been very limited. One example of connecting this gap was completed in the Amazon with an orbital hyperspectral sensor called Hyperion where an anthocyanin index was indicative of drought stress (Asner *et al.* 2004). To date, no one has developed a form of

anthocyanin detection using multispectral satellites which are more widely available. To be able to understand the challenges and implications of detecting anthocyanin by satellite, one must first understand how it is formed and why.

Anthocyanin

Anthocyanin is a member of a group of chemicals called flavonoids. Cyanidin-3-glucoside is the most common form of anthocyanin in leaves and accounts for more than 80% of all anthocyanins found in *Acer* leaves (Harborne 1967, Ribereau-Gayon 1972, Ji *et al.* 1992). These compounds are commonly found in cell vacuoles of the palisade and spongy mesophyll, but can be also found in the epidermis and hypodermis in some species (Gould and Quinn 1999, Burger and Edwards 1996) (Figure 1-1). Anthocyanin concentrations in sugar maple leaves can range from 1.5 to 48.2 nmol/cm^2 (Gitelson *et al.* 2001a); in this study, leaves with concentrations up to 28.8 nmol/cm^2 were found.

Figure 1-1. This is a cross section of a maple sugar leaf showing the location of anthocyanin—mainly in the palisade mesophyll (Photo credit: Harvard Forest 2009).
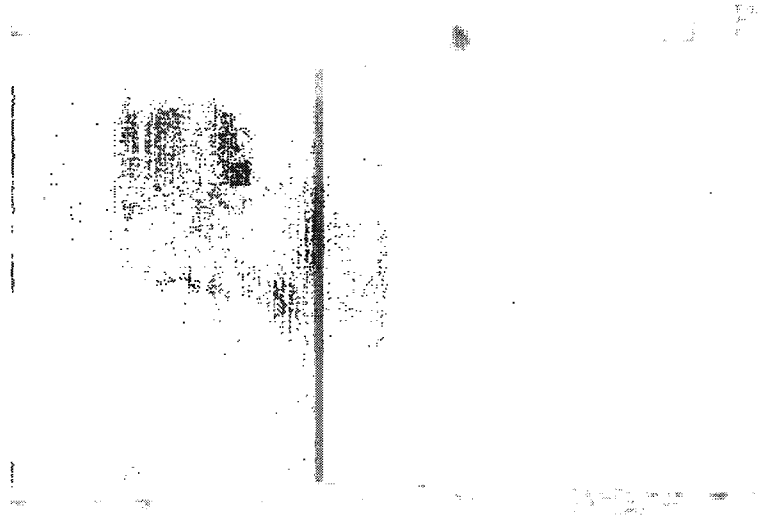
Anthocyanin Induction

In general, anthocyanin is present in areas where photosynthetic activity has decreased (Wheldale 1916). Yet it is not clear why anthocyanin is created. Is it a response to photoinhibition, carbohydrate overload, nutrient deficiencies, wounding, pathogen attack, herbivory, or osmotic stress? Or is it a response to symptoms caused by these situations? Below is a brief synopsis of different variables thought to induce anthocyanin synthesis.

Photoinhibiton and antioxidative properties.

Early investigations suggested that light is a stimulus for anthocyanin production, dependent on both intensity and duration (Wheldale 1916, Mancinelli 1983, Bowler *et al.* 1994, Krol *et al.* 1995). Many scientists believed that anthocyanin might protect against UV radiation through absorption, yet a universal theory of UV absorption is often discredited due to anthocyanin's high metabolic cost and relative inefficiency at UV absorption when compared to other flavonoids and phenolics (Caldwell *et al.* 1983, Teramura 1983, Beggs and Wellmann 1985, Takahaski *et al.* 1991, Stapleton and Walbot 1994, Brandt *et al.* 1995, Landry *et al.* 1995, Burger and Edwards 1996). A study by Feild *et. al.* (2001) showed that senescing red leaves were less photoinhibited and were able to function better than senescing green leaves. Some believe that photoprotection is the main role of anthocyanin, as it is the only member of flavonoid family to significantly absorb in the visible range (Shirley 1996).

Studies have investigated possible antioxidative properties of anthocyanin. Tsuda *et al.* (1996) found that introduced anthocyanins scavenged oxygen radicals. While

antioxidative activity is correlated with anthocyanin content in young leaves, it was weakly correlated in senescing leaves during the autumn. (van den Berg and Perkins 2007). There are many studies documenting the antioxidative properties of anthocyanin (Wang *et al.* 1997, Neill *et al.* 2002, Stintzing *et al.* 2002, Andersen and Markham 2006), but its importance in this role remains unclear.

Nutrient deficiency and carbohydrates.

During the fall, leaves start to remobilize many nutrients and elaborated compounds for export into storage, including nitrogen, phosphorus, potassium, and carbohydrates. There are several correlations between nutrient deficiencies and anthocyanin accumulation. Studies have found that low nitrogen concentrations are a stimulus for anthocyanin production (Hodges and Nozzolillo 1996, Kumar and Sharma 1999, Lee *et al.* 2003, Schaberg *et al.* 2003). While this can occur throughout the growing season, it is most readily seen in the fall as senescing leaves remobilize their nitrogen for storage (Himelblau and Amasino 2001, Hörtensteiner and Feller 2002). Phosphorus deficiencies have also been correlated with anthocyanin synthesis (Atkinson 1973, Trull *et al.* 1997, Zakhleniuk *et al.* 2001). In *Zea mays*, anthocyanin accumulation occurred in response to potassium deficiencies (Bhandal and Malik 1988).

Carbohydrates are also mobilized in the fall. Anthocyanin accumulation has been correlated with increased sugar concentrations in lab experiments (Overton 1899, Murray *et al.* 1994, Decendit and Mérillon 1996, Larronde *et al.* 1998), and in sugar maple leaves (Schaberg *et al.* 2003). In places that pool sugar naturally, such as girdling sites or after a

carbon sink is added, anthocyanin content increases (Hussey 1963, Jeannette *et al.* 2000) and when a carbon source is removed, anthocyanin concentrations decrease (Hussey 1963). It has been theorized that anthocyanin is produced in the autumn as a result of excess carbohydrates accumulating in leaves once the abscission layer has formed (Ishikura 1973, Kramer 1979).

Osmotic Stress.

During the fall, leaves are susceptible to frosts. Freezing creates cell damage through cellular rupture caused by ice crystals, and through dehydration as the availability of liquid water decreases (Chalker-Scott 1999). Anthocyanin production is induced by sudden cold temperatures (Nozzolillo *et al.* 1990, Christie *et al.* 1994, Leng *et al.* 2000). While many plants have frost hardiness mechanisms, anthocyanin has been implicated in providing immediate, temporary freezing tolerance rather than as an acquisition of hardiness (Steponkus and Lanphear 1969).

Osmotic stress as a result of drought also induces anthocyanin synthesis (see Chalker-Scott 1999 for review). Anthocyanin is found in plants that are more resistant to water stress (Knox 1989, Paine *et al.* 1992). Additionally, highly drought resistant resurrection plants experiencing dehydration accumulate three to four times more anthocyanin than is present in their hydrated state (Sherwin and Farrant 1998). An increase in solutes plays an active role in osmotic stress, giving this possibility credence.

Wounding, Pathogens, and Herbivory.

Anthocyanin production has been hypothesized as a response to herbivory, wounding, and pathogen attacks. It is speculated that anthocyanin biosynthesis is a herbivory resistant modification, which Coley and Aide (1989) showed by finding that leaf cutter ants were deterred by higher anthocyanin contents. Yet, others have found that anthocyanin does not inhibit feeding (Quiros *et al*. 1977, Isman and Duffey 1982). Anthocyanin also does not have any toxic or deterrent properties (McClure 1975, Lee 1987), although some have postulated these properties exist (Janzen 1979, Hamilton and Brown 2001). It seems that animals may respond to anthocyanin as an indicator of other leaf characteristics, versus reacting directly to anthocyanin (Close and Beadle 2003).

Autumnal Response.

Autumn pigments can be seen as a result of preferential degradation of chlorophyll (Goodwin 1958, Lichtenthaler 1987). Carotenoids degrade more slowly than chlorophyll, therefore leaves with high carotenoid content look orange or yellow in the fall (Keskitalo *et al*. 2005). Chlorophyll degradation contributes to the visibility of these other pigments, including anthocyanin, which can be synthesized in the fall. Within a tree, anthocyanin development varies. In maples, parts of the tree that are most exposed to sunlight tend to turn color first and therefore color progresses from the upper crown downward and inward (Chang *et al*. 1989). Anthocyanin does not typically accumulate in shaded leaves; this is most easily seen in the contrast between overlapping leaves (Kozlowski and Pallardy 1997). In aspens, once anthocyanin synthesis had begun it was correlated with excess light conditions, frost, and cold, clear days but was negatively correlated to

rainy days (Keskitalo *et al*. 2005). Others suggest that synthesis is associated with warm autumn days, cool nights without killing frosts and several years of relatively high precipitation (Cottam 1966). Kozlowski and Pallardy (1997) suggest that clear skies, cool temperatures and mild drought conditions would induce the most anthocyanin. Overall, many environmental factors have been implicated in anthocyanin synthesis. There are many anecdotal conditions that people associate with the most vibrant autumn colors. Further investigation is needed to quantify these variables and their role in autumn foliage. Although the exact causes of anthocyanin production remain to be determined, their occurrence during autumnal senescence in maples is well documented and diagnostic of the senescence process.

Climate change will affect fall foliage by changing the conditions which contribute to anthocyanin synthesis. Increased temperatures in the fall are associated with muted foliage colors (NECIA 2006, NERA 2007). The predicted increase of drought in the summer and fall will possibly decrease leaf color expression (NECIA 2006). An extension of the growing season may also affect foliar displays by changing the timing and duration of a favorable temperature regime. In one experiment an increase of 4°C caused an extension of the growing season by 17-24 days (Norby *et al*. 2003). Rising temperatures will also delay leaf abscission. When sugar maple and red maple were examined on the same day, there was a 21%-74% difference in percent leaf abscission between the increased temperature treatment and the control (Norby *et al*. 2003). The sugar maples and red maples are also in danger of disappearing as dominant species types as their habitat shifts –as shown by both the low emissions and high emissions

scenarios examined by the US Global Change Research Program (Barron 2001, Iverson and Prasad 2001).

Spectral Characteristics

All flavonoids absorb radiation. The absorption shifts from UV toward visible light with increasing modification within the flavonoid pathway (Swain 1965). Anthocyanin is the most complex flavonoid and the only one to absorb significantly in the visible spectrum (Harborne 1967, Shirley 1996). Figure 1-2 illustrates anthocyanin's reflectance spectrum. *In vivo* absorption is centered at 550nm and is strongly related to anthocyanin content (Harborne 1967, Nakayama and Powers 1972). Broadband absorption occurs to some degree due to internal reflection, scattering, and unhomogenous distribution of the anthocyanin pigment within a leaf (Rabinowitch 1945, Fukshansky *et al*. 1993). Anthocyanin can affect the red edge at high concentrations and cause it to be independent of chlorophyll concentration, although at low concentrations the relationship between chlorophyll and red edge is linear (Curran *et al*. 1991). Others have found that anthocyanin does not affect the red edge properties at all and when comparing anthocyanic and non-anthocyanic leaves both absorb similarly in the blue, red, and near-infrared regions (Gitelson *et al*. 2001a). While Figure 1-3 shows some shift in the red edge inflection point (REIP), further investigation is needed to determine if this response is due to anthocyanin.

To create a spectral index, anthocyanin's highest absorption at 540-550nm is the best place to start (Figure 1-2) (Gamon and Surfus 1999, Merzlyak and Chivkunova 2000,

Gitelson *et al.* 2001a). Unfortunately, the 550nm range is also strongly affected by chlorophyll. Many studies have identified the 700nm band as having approximately equal reflectance to the 550nm range for chlorophyll and since anthocyanin does not affect this band it has been proposed for use as an approximation for green reflectance due to chlorophyll (Gitelson *et al.* 2001a, Gitelson *et al.* 2001b, Sims and Gamon 2002, Merzlyak *et al.* 2003).

Figure 1-2. Reflectance measurements from wine grapes (*Vitis vinifera* L.) with different anthocyanin concentrations. As anthocyanin concentrations increase there is increased absorption in the green wavelengths. At higher concentrations, anthocyanin influence can be seen in the red wavelengths (640nm)—although this is not where the greatest change in reflectance occurs. Lines indicate 550, 640, and 700nm. Adapted from Agati *et al.* (2007).
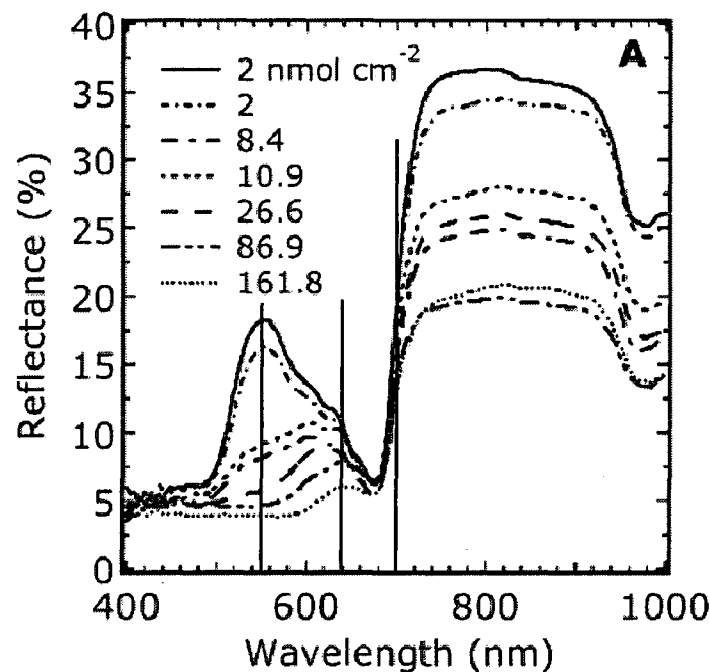
Thus, the difference between reflectance at 550nm and 700 nm would calculate the absorption solely due to anthocyanin. In fact, this index has been used and found to be sensitive even at minute anthocyanin concentrations—as low as 1-2 $nmol/cm^2$ (Merzlyak *et al.* 2003). The differences in the leaf spectra from green versus red leaves can be seen

in Figure 1-3. This graph shows how these different band locations change with changing anthocyanin and chlorophyll concentrations.

While studies have shown a correlation between the red:green ratio and anthocyanin (Gamon and Surfus 1999), this relationship is weak when applied to multiple species (Gitelson *et al.* 2001a, Sims and Gamon 2002). While this may be useful in certain circumstances, more broadly applicable equations can be used, as seen below. Anthocyanin estimation can be made using bands in the 550nm, 640nm, 700nm, and a near infrared (NIR) component (750nm and above) to normalize for leaf structure.

Figure 1-3. Example of VIRIS results. A= anthocyanin concentration (mg/cm^2), C= chlorophyll concentration (mg/cm^2). Curves are from varying dates and cover a range of anthocyanin and chlorophyll concentrations. Shaded sections show areas of interest for anthocyanin indices.
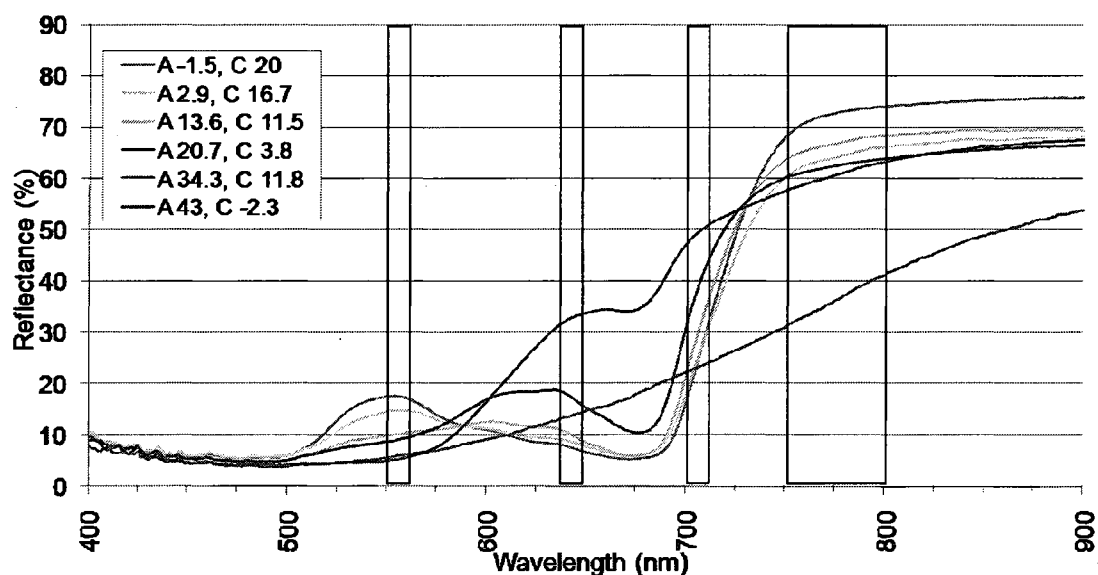
Below are several versions of the Anthocyanin Reflectance Index (ARI) (Gitelson *et al.* 2001a). In the equations below "R" is reflectance and R_{nir} is reflectance from 750-800nm:

Equation 1. ARI= $(1/R550 - 1/R700) * R_{nir}$ STD 3.9 nmol/cm^2 (Gitelson *et al.* 2001a)

Equation 2. ARI= $(1/R(530-570) - 1/R(690-710)) * R_{nir}$ STD unknown, where each reflectance component has a range of possible wavelengths that can be used for estimation (Gitelson *et al.* 2006).

This index changes as anthocyanin concentrations increase. Merzlak *et. al.* (1997) found that the index saturates at 40-50nmol/cm^2. After 25nmol/cm^2 switching to a single band, 1/R550 (or R_{nir} /R550), proves to be more accurate (Gitelson *et al.* 2001a).

Another anthocyanin index is created with a ratio between red and green wavelengths (Equation 3). This index has been found to detect anthocyanin in Coast live oak (*Quercus agrifolia*), yet in other tests with a multitude of species it was found to be not well correlated (Gamon and Surfus 1999, Sims and Gamon 2002).

Equation 3. Red:Green $= \dfrac{\sum\limits_{i=600}^{699} Ri}{\sum\limits_{i=500}^{599} Ri}$ where R is reflectance (Sims and Gamon 2002).

Remote Sensing Systems

Remote sensing allows for rapid, non-destructive analysis of pigments in plants distributed over a large area. Satellite systems acquire whole-canopy views that are otherwise very difficult to obtain. Not only does this process often reduce costs, it also

allows for large area analyses and repetitive visits to the same site that have not been altered by field tests. Remote sensing also allows for larger scale hypothesis testing and incorporates a whole-ecosystem approach (Ustin *et al.* 1993). Development of indices and determination of spectral features has allowed scientists to determine more than just the reflectance of light—such as water stress and species type (Ustin *et al.* 2004). In fact, scientists can now determine specific concentrations of leaf components, such as nitrogen (Smith *et al.* 2003). Being able to deduce concentration levels of pigments from remote sensing allows insight into the physiological characteristics of a plant community. Several different orbital platforms for remote sensing are available. In this study laboratory VIRIS measurements as well as space-borne Hyperion, MERIS, Landsat TM/ETM+, and MODIS data will be evaluated.

VIRIS

The GER 2600[1], a VIRIS (Visible IR Intelligent Spectrometer), is a remote sensing field instrument that measures 512 bands within the electromagnetic spectrum. In this study, it was used in a laboratory setting where the field of view is approximately $4cm^2$ and allows for individual leaf determination. The VIRIS covers a spectral range of 400-2800nm with a spectral resolution of 2nm for the part of the spectrum used in this study (400-1000nm); a Spectralon-coated hemispherical illumination systems was used (Vogelmann *et al.* 1993). It has been found that approximately 80% of the light reflected can be attributed to the top leaf when leaves are in stacks of seven (Vogelmann *et al.* 1993,

---

[1] The use of specific brand names is for clarity only and does not imply endorsement.

Rock *et al.* 1994). Reflectance measurements from this instrument can be used to characterize differences through fall senescence as seen in Figure 1-3.

Satellite Systems

Hyperion.

Launched in November of 2000, Hyperion is a satellite sensor on board NASA's EO-1 which acquires hyperspectral images of the Earth from orbit. 'Hyperion has 220 spectral bands ranging from 350nm to 2500nm with a resolution of 10nm. One image is 7.6km wide with a length of 42 or 185 km, and a spatial resolution of 30 meters. Hyperion images must be ordered before image acquisition occurs.

MODIS.

MODIS (Moderate Resolution Imaging Spectroradiometer) is a multispectral imaging sensor on NASA's Terra (it is also on Aqua) platform launched in December of 1999. Its images have a swath width of 2,330km. Its nadir spatial resolution varies from 250m to 1000m. This system has 36 spectral bands. It can revisit a site every one to two days. Bands with a spatial resolution of 1000m are MODIS ocean bands. Bands useful for this study include (* denotes most useful bands):

Table 1-1. Spectral bands for MODIS.

Band	Bandwidth Wavelengths (nm)	Color	Spatial Resolution (m)
*Band 1	620-670	Red	250
*Band 2	841-876	NIR	250
Band 3	459-479	Blue	500
*Band 4	545-565	Green	500
Band 8	405-420	Blue	1000
Band 9	438-448	Blue	1000
Band 10	483-493	Yellow	1000
Band 11	526-536	Green	1000
*Band 12	546-556	Green	1000
Band 13	662-672	Red	1000
Band 14	673-683	Red	1000
*Band 15	743-753	NIR	1000
Band 16	862-877	NIR	1000
Band 17	890-920	NIR	1000

MERIS.

MERIS (Medium Resolution Imaging Spectrometer) is operated by the European Space Agency (ESA) and was launched in March of 2002. It has 15 bands with narrow spectral resolution between 2.5nm and 10nm. Its images have a swath width of 1150km. It can obtain global coverage every three days. Bands include (* denotes most useful bands):

Table 1-2. MERIS spectral bands.

Band	Bandwidth		Spatial
Band 1	407.5-417.5	Blue	300
Band 2	437.5-447.5	Blue	300
Band 3	485-495	Yellow	300
Band 4	505-515	Green	300
*Band 5	555-565	Green	300
Band 6	615-625	Red	300
Band 7	660-670	Red	300
Band 8	677.5-685	Red	300
*Band 9	700-710	Red	300
Band 10	750-757.5	NIR	300
*Band 11	758.75-761.25	NIR	300
Band 12	767.5-782.5	NIR	300
Band 13	855-875	NIR	300
Band 14	885-895	NIR	300
Band 15	895-905	NIR	300

Note that Band 5, Band 9, and Band 11 align with parameters set forward by Gitelson *et al.* (2006) for anthocyanin estimation.

Landsat TM/ETM+.

Various forms of the Landsat sensor have been used since the first went up in July of 1972. The bands found on Landsat TM/ETM+ (Enhanced Thematic Mapper), are used in this study. Landsat TM/ETM+ pixels have a spatial resolution of $30m^2$ and are acquired every 16 days for the same point on the ground. The spectral resolution changes from 60nm to 210nm depending on which of the seven bands is considered. Bands used include (* denotes most useful bands):

Table 1-3. Landsat TM/ETM+ spectral bands.

Band	Bandwidth Wavelengths (nm)	Color	Spatial Resolution (m)
Band 1	420-520	Blue	30
*Band 2	520-600	Green	30
*Band 3	630-690	Red	30
*Band 4	760-900	NIR	30

Hypotheses

H1- A laboratory-derived spectral index will detect and characterize the amount of anthocyanin within sugar maple leaves during fall senescence.

H2- Based on laboratory studies, an anthocyanin index can be extrapolated into multispectral form for use with multispectral satellites.

H3- Satellite-based ARI data will provide an accurate portrayal of anthocyanin development during senescence.

Objectives

1. Determine how anthocyanin concentration affects the spectral characteristics of sugar maple leaves. Use this information to compare extracted anthocyanin concentrations with published hyperspectral indices and create new indices if necessary.

2. Simulate satellite bands from hyperspectral data and create simulated satellite anthocyanin indices for Hyperion, MODIS, Landsat TM/ETM+ and MERIS. Compare these results to hyperspectral indices and determine the ability of these satellites to detect anthocyanin.

3. Using the satellite indices developed from objective 2, apply the indices to acquired satellite imagery to see if an autumnal signal can be detected from space-borne imagery.

CHAPTER 2

DEVELOPING A HYPERSPECTRAL ANTHOCYANIN INDEX FOR SUGAR

MAPLE LEAVES

Abstract

Development of hyperspectral indices for providing quantitative analysis of anthocyanin

is an alternative to destructive laboratory measurements. Anthocyanin, a red pigment

produced by many plant species, has been recognized as an indicator of plant stress.

Remote detection and quantification of this pigment could be used to assess the health

and status of plants efficiently and over large areas. Reflectance measurements were

compared to test pigment extractions to develop hyperspectral anthocyanin indices for

sugar maple trees. Red reflectance was not well correlated to anthocyanin concentration

so absorption at R550nm was targeted, yet this wavelength is complicated by reflectance

of chlorophyll; the best estimation to remove this effect was using the reciprocal of

reflectance in the red edge region. Laboratory results indicated that absorption at 564nm

and reflectance at 697nm estimate anthocyanin concentrations best, which are within the

wavelength range of published indices.

Introduction

Anthocyanin is formed in reaction to many different types of stresses including photoinhibition, oxidative and osmotic stress, nutrient deficiency, and wounding (Chalker-Scott 1999, Close and Beadle 2003, Gould 2004). Due to anthocyanin's response to a wide range of plant conditions, it can be used as a general indicator of plant stress (Andersen and Markham 2006). Anthocyanin development in the fall, a well-known phenomenon in New England, is due to photoinhibition as chlorophyll is actively degraded during senescence. The senescence process produces the brilliant fall colors and is responsible for over a billion dollars in annual direct spending in New Hampshire alone (Development 2007). Tracking fall foliage change through laboratory analysis of pigments is time consuming and its scope is limited. Developing a hyperspectral index to broaden the ability to measure anthocyanin using remote sensing methods is necessary in order to measure foliar color changes and intensities at a greater scale.

While anthocyanin is seen visibly as red, reflectance at this wavelength is not correlated to concentration (Curran *et al.* 1991, Neill and Gould 1999). Therefore, scientists have developed spectral indices based on anthocyanin's absorption characteristics (Gamon and Surfus 1999, Merzlyak and Chivkunova 2000, Gitelson *et al.* 2001a). As the most modified flavonoid, anthocyanin absorbs significantly in the green (Harborne 1967, Shirley 1996). Yet chlorophyll reflects in the green and therefore its signal needed to be subtracted in order to detect absorption due to anthocyanin. Chlorophyll's reflectance at 550nm (R550) is typically estimated by the reciprocal of reflectance values from the red and near infrared wavelengths (Sims and Gamon 2002, Gitelson *et al.* 2001a, Merzlak *et*

al. 1997). There are a number of chlorophyll indices that are based on red-edge reflectance which may estimate R550 as well (Chappelle *et al.* 1992, Vogelmann *et al.* 1993, Gitelson and Merzylak 2004). Putting these terms together to form an anthocyanin reflectance index (ARI) yields:

Equation 1. $ARI = 1/\lambda_{green} - 1/\lambda_{red\ edge}$ (Gitelson *et al.* 2001a)

Most anthocyanin indices fall into two or three band spectral models. The three components in the equation include reflectance in the green which is a dual signal containing both anthocyanin absorption and chlorophyll reflectance, the red edge component which subtracts the contribution of chlorophyll reflectance at 550nm, and the near infrared component which is added to account for differences in leaf structure (Equation 2) (Myers 1970). An additional term, the log of R550, was tested to account for the non-linear relationship between concentration and reflectance (Equation 3) (Buschmann and Nagel 1993, Blackburn 1999).

Equation 2. $ARI_{nir} = (1/\lambda_{green} - 1/\lambda_{red\ edge}) * \lambda_{near\ infrared}$ (Gitelson *et al.* 2001a)

Equation 3. Concentration based $ARI = (1/\lambda_{green} - 1/\lambda_{red\ edge}) * \log(\lambda_{green})$

Where λ_{green} is 530-570nm, $\lambda_{red\ edge}$ is 690-710nm, and $\lambda_{near\ infrared}$ is 750-800nm (Gitelson *et al.* 2006, Merzlyak *et al.* 2003).

Another anthocyanin index which employs the red region by creating a ratio (Equation 4) will also be tested in this study. This index has been found to detect anthocyanin in Coast

live oak (*Quercus agrifolia*), yet in other tests with a multitude of species it was found to be not well correlated (Gamon and Surfus 1999, Sims and Gamon 2002).

$$\text{Equation 4. Red:Green} = \frac{\sum_{i=600}^{699} Ri}{\sum_{i=500}^{599} Ri} \quad \text{where R is reflectance (Sims and Gamon 2002).}$$

The objective of this study is to take a new approach in developing a spectral index to determine which anthocyanin index best applies to sugar maples as they are a dominant tree type and one of the consistent anthocyanin producers in the Northeast. Anthocyanin is actively produced in sugar maples during the fall, therefore providing a unique opportunity for tracking senescence and for testing various published and unpublished anthocyanin indices. As sugar maple trees turn red in the fall, the remote sensing of this pigment could be a powerful objective indicator of fall foliar color development. Such remote sensing methods could then be used in assessing changes in the character of fall color displays across the northeast which may be related to altered climatic conditions over time.

Methods

Ten sugar maples tree located near Durham, NH were sampled weekly (9/2, 9/9, 9/16, 9/23, 9/30, 10/7, 10/14, 10/21, 10/28) over the fall of 2008, resulting in over 700 leaf samples—of which 25 leaves representative of a range of anthocyanin concentrations were selected for pigment extractions. The trees were sampled in the morning, from the southern aspect, in the lower two thirds of the outer canopy (van den Berg and Perkins

22

2007). Leaves from each tree were placed in a Ziplock bag with a wet paper towel and stored in a cooler supplied with frozen blue ice until measured. Each leaf was measured three times using a Visible/Infrared Imaging Spectrometer (VIRIS) with a field of view of 4.0cm^2 (GER 2600[1], Geophysical and Environmental Research Corporation, Millbrook, NY), in progressive 90 degree rotations, for an average reflectance value (Rock et al. 1986, Vogelmann et al. 1993, Soukupová et al. 2002). Leaves were then frozen at -80°C until used for pigment extractions (Schmitzer et al. 2009, Ehlenfeldt and Prior 2001).

Ten leaf punches (1.58 cm^2 each) were taken from the area measured by the VIRIS and ground with a mortar and pestle in 100% methanol until white. Samples were then centrifuged for 5 minutes. Part of this supernatant was used for chlorophyll extractions and concentrations were calculated from equations created by Lichtenthaler (1987). The remaining solution was then used for anthocyanin extraction by adding 0.1% (v/v) of 12.1M HCl (Murray et al. 2003). All samples were measured for absorbance using a Cary 50 spectrophotometer[1]. Anthocyanin concentrations were calculated using standard methods and an extinction coefficient of 30,000 mol^{-1} cm^{-1} (Steele et al. 2008, Murray et al. 2003).

The July collections used for the chlorophyll index test were sampled on 7/11/2008 and 7/29/2008 at Foss Farm in Durham, NH. They were measure with the VIRIS as noted above; chlorophyll extractions occurred the same day using 10 leaf punches, 95%

---

[1] The use of specific brand names is for clarity only and does not imply endorsement.

ethanol, and an incubation time of 16 hours following the methods of Minoscha *et al.* 2009. Chlorophyll values were calculated using Lichtenthaler 1987.

Food coloring was used to test the relationship between concentration and reflectance. Reflectance measurements were taken using the VIRIS after each addition of one drop of green food coloring (manufactured by McCormick) to 10mL of water in a petri dish. A petri dish with 10mL of water was used as a reference.

Results and Discussion

Anthocyanin values between 0 and 28.8 nmol/cm^2 were found in sugar maples leaves which is consistent with published values (Steele *et al.* 2008, Gitelson *et al.* 2001a). Most anthocyanin develops after chlorophyll levels have dropped below 10 mg/cm^2.

Some pigment concentrations, such as chlorophyll, can be estimated by the amount of light they reflect (Gitelson and Merzylak 2004, Datt 1998). To estimate anthocyanin this way would require measuring the reflectance of red light. When anthocyanin concentrations are compared to reflectance in the red and red edge wavelengths there is moderate correlation (Figure 2-1), yet this relationship is dominated by several low anthocyanin leaves (highlighted) (Figure 2-2). There is not much of a correlation between red light and anthocyanin concentrations when you focus on those leaves with more than 6nmol/cm^2 (unhighlighted points in Figure 2-2).

The anthocyanin index based on reflectance in the red and green (Equation 4), was correlated with anthocyanin concentrations ($r^2 = 0.83$) when considering all leaves (Table

2-2). While this relationship provides a good fit, better estimation of anthocyanin using

the absorption characteristics of this pigment may be possible.

Figure 2-1. Correlation of red and red edge wavelengths (600-720 nm) with varying
amounts of anthocyanin concentrations (0-28.8 nmol/cm2) using the Pairwise method.
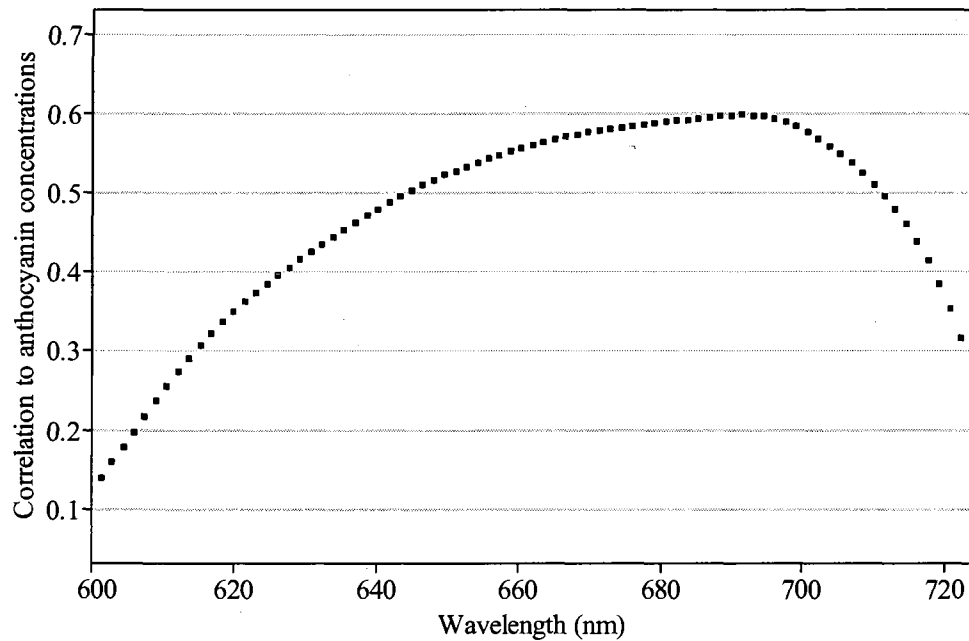
Figure 2-2. Anthocyanin concentrations versus red light. Highlighted points represent 7
observations with low amounts of anthocyanin. These points dominate the relationship
plotted in Figure 2-1.
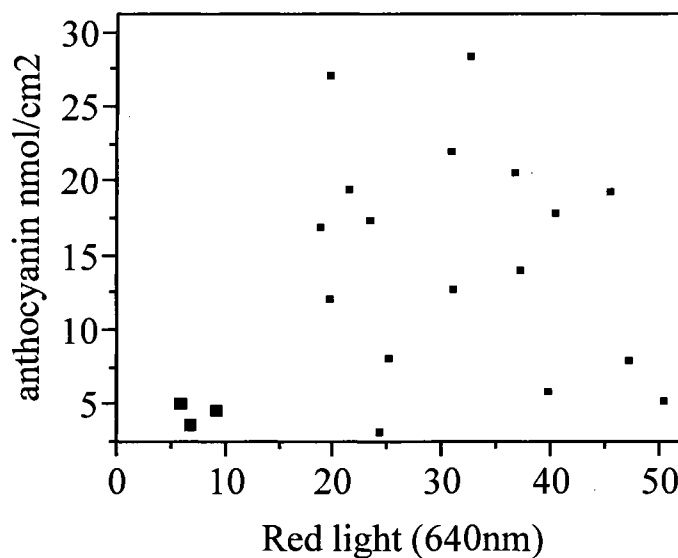
Anthocyanin absorbs in the green region of the EM spectrum with a peak at 550nm in vivo. Yet, this is also where chlorophyll reflects. Figure 2-3 shows these relationships visually by comparing two leaves with similar chlorophyll concentrations but different anthocyanin concentrations ; the bold line represents a leaf with less anthocyanin ($3nmol/cm^2$) than the dotted line ($13 nmol/cm^2$) (concentrations estimated by anthocyanin index (Gitelson *et al.* 2001a)), both have approximately $11 nmol/cm^2$ of chlorophyll (chlorophyll index (Gitelson and Merzlyak 2004)). Notice the difference between the spectral curves is most noticeable in the green.

The overlapping signals of chlorophyll reflectance and anthocyanin absorption must be separated. To attempt this, several relationships were examined to estimate chlorophyll's contributions to the reflectance at 550nm including published chlorophyll indices such as the red edge inflection point (REIP), and reciprocal reflectance in the red and red edge wavelengths (Gitelson and Merzylak 2004, Vogelmann *et al.* 1993, Sims and Gamon 2002).

Several published chlorophyll indices can predict the amount of chlorophyll present in the fall leaves well (Table 2-1), yet correlating concentration to the amount of reflectance at 550nm is more difficult due to the dual signal present in the fall leaves. A separate database of leaves collected in July was used to correlate R550 to chlorophyll indices. These leaves have little to no anthocyanin and therefore reflectance at 550nm is assumed to be solely attributed to chlorophyll. The best chlorophyll index for use in the

ARI was determined by comparing how well it correlates to chlorophyll concentrations in the fall leaves and how well it correlates to R550 in green summer leaves.

Figure 2-3. This example shows two leaves with similar chlorophyll concentrations but differing anthocyanin concentrations. The dotted line represents a leaf with more anthocyanin. Note the difference in green reflectance and lack of difference in the red wavelengths (600-699 nm).
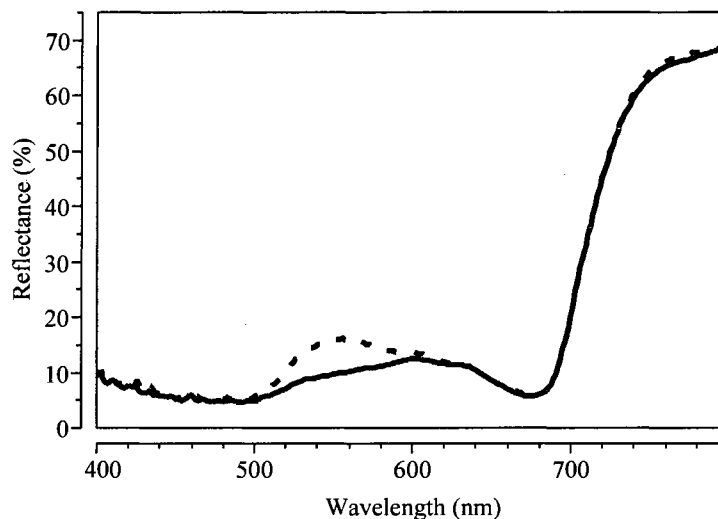
Most chlorophyll indices correlated well with extracted chlorophyll concentrations, most notably R695/R760 (Carter 1994), R710/R760 (Carter 1994), R750/R700 (Gitelson and Merzylak 2004), and RE3/RE2 (Vogelmann *et al.* 1993) (Table 2-1). The indices which correlated best with R550 summer leaves were TCARI—transformed chlorophyll absorption reflectance index (Kim 1994), R710 (Gitelson *et al.* 2006), R700 (Gitelson *et al.* 2006), first derivative of R705 (Vogelmann *et al.* 1993), and Datt (1998) (Table 2-1). None of these match the best indices for detecting chlorophyll concentrations. Most indices which performed well in matching R550 in the green summer leaves, do not perform as well with the extracted chlorophyll values in the fall leaves. The REIP correlates well with extracted values, but is not correlated with R550 and therefore would

not be a very good estimator of chlorophyll's reflectance at R550 (Table 2-1). The best

correlations when considering both relationships occur with reciprocal reflectance of the

red edge wavelengths (Table 2-1); R700 had the highest correlations for both

relationships and therefore will be used as the best estimation of chlorophyll's reflectance

at R550. This relationship and use of R700 has been recommended and used in several

anthocyanin indices (Gitelson *et al.* 2001a, Merzlyak *et al.* 2003).

The correlation between anthocyanin concentration and Gitelson's ARI (Equation 1) for

sugar maple was significant (r^2=0.91) (Table 2-2 and Figure 2-4).

There are many wavelengths that can be used for the different components of the ARI;

R550 can be substituted with 540-570nm and R700 with 690-710nm (Gitelson and

Merzlyak 2004, Gitelson *et al.* 2006). Other ARI combinations were tested using these

various wavelengths, and the best correlation occurred when using R564 and R697

(Table 2-2). These values were not the most correlated for either individual component,

yet combined as an index it yields a slightly higher correlation than the ARI ($r^2 = 0.916$).

Modifications of the ARI (Equation 1) have also been studied by using a near infrared

term to account for differences in leaf structure (Equation 2). In comparison to the

extracted values, this addition provided similar results to the ARI but decreased slightly

in correlation (Table 2-2). A more dramatic increase in fit may occur in experiments

dealing with multiple species, but this study used leaves from a single species which may

have led to the apparent reduced influence of structure on anthocyanin determination

(Gitelson *et al.* 2006).

Table 2-1. Correlation of chlorophyll indices to chlorophyll concentrations in fall leaves and to R550 in green summer leaves. Indices are identified by author and reflectance values used. Root mean square error (RMSE) for chlorophyll concentrations is in mg/cm^2; RMSE for R550 is in % reflectance.

Index	Type of Fit	r^2	RMSE	r^2 to R550	RMSE
Carter 695,760	reciprocal	0.984	17.63	0.594	0.895
Carter 710,760	reciprocal	0.978	20.67	0.703	0.765
Carter 605,760	reciprocal	0.909	42.26	0.788	0.646
Gitelson 750,700	reciprocal	0.985	17.33	0.719	0.744
Chappelle 675,650,700	reciprocal	0.479	100.89	0.479	1.013
Chappelle 675,700	reciprocal	0.888	46.79	0.607	0.881
Vogelmann RE3/RE2	linear	0.973	22.85	0.670	0.806
First derivative 715	exponential	0.885	47.36	0.524	0.969
First derivative 705	exponential	0.481	100.66	0.850	0.543
Vogelmann Fd715,fd705	linear	0.297	117.20	0.667	0.810
Kim TCARI 550,670,700	linear	0.250	121.04	0.933	0.362
Huete OSAVI 670,800	quadratic	0.892	47.06	0.024	1.387
Gitelson 705-750	linear	0.947	32.74	0.717	0.746
Gitelson 694-740, 750-800	linear	0.951	30.59	0.615	0.871
Datt 550,680,708	reciprocal	0.533	95.52	0.840	0.562
Gitelson 690-720,760-800	linear	0.975	21.91	0.655	0.825
Vogelmann REIP	linear	0.912	41.36	0.172	1.278
Asrar NDVI 630-690,760-900	quadratic	0.933	37.07	0.252	1.214
Red Edge 3/1 695-705,734-746	linear	0.982	18.60	0.693	0.778
R691	reciprocal	0.952	30.65	0.410	1.078
R693	reciprocal	0.953	30.45	0.576	0.914
R695	reciprocal	0.951	30.96	0.702	0.702
R696	reciprocal	0.947	32.16	0.777	0.770
R697	reciprocal	0.942	33.78	0.819	0.819
R699	reciprocal	0.935	35.63	0.845	0.845
R700	reciprocal	0.924	38.41	0.861	0.523
R710	reciprocal	0.708	75.47	0.878	0.491

It is interesting to note that as chlorophyll concentrations get higher (above 10mg/cm^2), the ARI underestimates the amount of anthocyanin slightly more than overestimates it, both in the number of observations and in value (Figure 2-5).

Figure 2-4. Correlation between extracted anthocyanin concentrations and the hyperspectral index ARI (Equation 1).
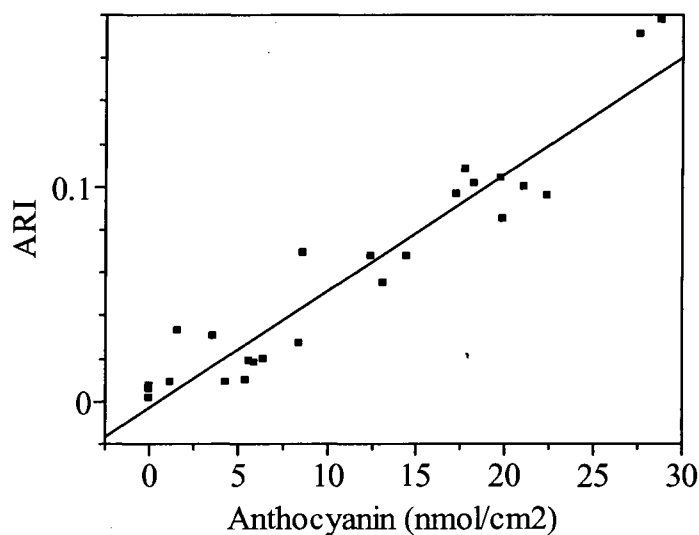
Table 2-2. Correlation and root mean square error (RMSE) of several hyperspectral indices to estimate anthocyanin concentration.

Index	r^2	RMSE
ARI (1/R550-1/R700)	0.910	7.76
ARI$_{nir}$ ((1/R550-1/R700)* R750)	0.909	7.85
ARI with log ((1/R550-1/R700)* logR550)	0.914	7.612
Red:green ($\sum\limits_{i=600}^{699} Ri$ / $\sum\limits_{i=500}^{599} Ri$)	0.827	10.81
1/R564- 1/R697	0.916	7.54

Figure 2-5. Residual plot of the fit line in Figure 2-4. Bold points indicate chlorophyll concentrations over 10 mg/cm^2.
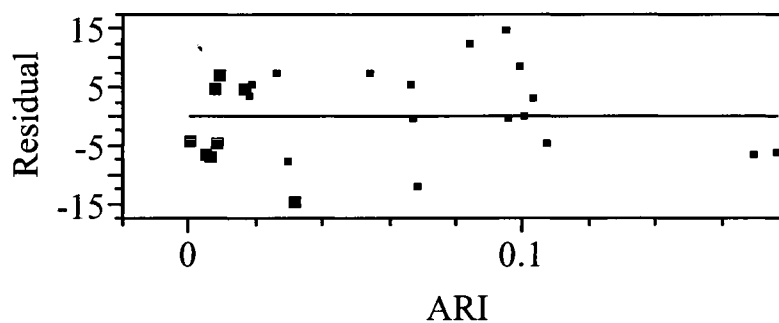
This may be due to the ratio of the pigments. It is difficult to detect small amounts of anthocyanin when chlorophyll concentrations are high—as this small addition is masked by the chlorophyll which affects the reflectance strongly. The ARI is based on linear relationships, but concentration and reflectance follow a logarithmic relationship at high values (Figure 2-6). As concentrations get higher, the amount of pigment that is added affects the overall reflectance less. To account for the fact that overall concentration of the combined pigments will reduce reflectance in the green peak, both by a reduction in reflectance by chlorophyll as the leaves become a darker green and by an increase in the absorption of anthocyanin, one can multiply the ARI by the log of R550 (Equation 3). This equation increased the correlation with anthocyanin concentrations slightly (Table 2-2).

Figure 2-6. Correlation between reflectance and concentration. Results based on food coloring test. A log fit is shown, r^2=0.99.
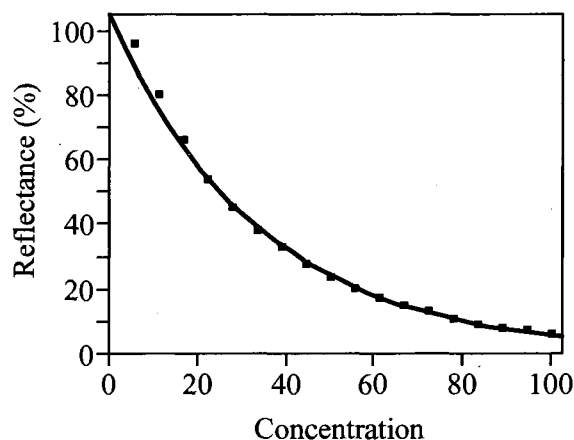
When the concentration-based ARI index was tested on a separate database based on grapevine leaves it improved the correlation, but it was not a significant increase (Steele 2009). This factor may be useful for other datasets, particularly ones with higher total pigment concentrations of both anthocyanin and chlorophyll.

Conclusions

The anthocyanin hyperspectral index which performed best overall was (1/R564-

1/R697). The use of a near infrared component to estimate for structure did not increase

the correlation with anthocyanin concentrations; the use of the log to account for the

relationship between concentration and reflectance increased correlation slightly. The

lack of a unique reflectance signature at any single point in the visible wavelengths

constrains the ability to remotely sense anthocyanin, and also to detect beginning

development of the pigment if it occurs in leaves with high chlorophyll concentrations.

Yet, for fall foliage where chlorophyll levels are naturally lowered, the current study has

shown that this hyperspectral index performs well and could be used as a means of

measuring anthocyanin concentrations non-destructively.

CHAPTER 3

SIMULATING SATELLITE ANTHOCYANIN INDICES AND COMPARING THEIR

CORRELATION TO HYPERSPECTRAL ANTHOCYANIN INDICES

Abstract

Anthocyanin is a red pigment that is indicative of many types of plant stress. By

developing effective spectral indices for detecting changes in anthocyanin concentrations,

such indices can quantify pigments non-destructively and across a multitude of spatial

and temporal scales. Plant pigment indices have been derived using hyperspectral and

multispectral data which are useful for applications with satellite sensors. Yet, to date,

there is not a multispectral anthocyanin index. This paper compares hyperspectral indices

to simulated satellite indices for use with Hyperion, MERIS, MODIS, and Landsat

TM/ETM+ using laboratory-based VIRIS data. Results show that all satellites have some

predictive power for detecting anthocyanin with the most consistent performance

associated with a red:green spectral ratio.

Introduction

Anthocyanin is a red pigment found in many plant species and can be seen throughout

New England during the autumn. Anthocyanin has been shown to be a universal

indicator of plant stress formed in response to a number of conditions including

photoinhibition, oxidative and osmotic stress, nutrient deficiency, and wounding. Detecting its presence would therefore be useful for ecosystem analysis and characterization as well as for monitoring changes during autumn senescence over the past several decades.

Climate change will affect fall foliage by changing the conditions which contribute to anthocyanin synthesis. Increased temperatures in the fall are associated with muted foliage colors (NECIA 2006, NERA 2007). The predicted increase of drought in the summer and fall will possibly decrease leaf color expression (NECIA 2006). Sugar maples are also in danger of disappearing as a dominant species type as their habitat shifts –as shown by both the low emissions and high emissions scenarios examined by the US Global Change Research Program (Barron 2001, Iverson and Prasad 2001). Plant pigments react to environmental stresses, such as those induced by climate change. It may be possible to track stress to sugar maples, and other species, if a satellite-based anthocyanin index is developed.

The most accurate way to measure pigment concentrations is through destructive analysis, yet development of non-destructive assessment methods through the use of remote sensing have been used as a proxy for estimating concentration. Absorption and reflectance features have been characterized for many pigments and spectral indices have been created to eliminate overlap between different pigment features (Merzylak *et al.* 1999, Gitelson and Merzylak 2004). Hyperspectral indices for anthocyanin have been developed by previous research using a two or three band ratio. A band, λ_{green}, accounts

for anthocyanin absorbance and chlorophyll reflectance, while the band $\lambda_{red\ edge}$ estimates

chlorophyll's reflectance in the λ_{green} region. By subtracting the $\lambda_{red\ edge}$ from λ_{green} the

result is an anthocyanin signature; some indices also include a band in the near infrared to

account for leaf structure (Merzylak 1999, Gitelson *et al.* 2001a, Sims and Gamon 2002,

Gitelson *et al.* 2006). The resulting equations are:

Equation 1. $ARI = 1/\lambda_{green} - 1/\lambda_{red\ edge}$ (Gitelson *et al.* 2001a)

Equation 2. $ARI_{nir} = (1/\lambda_{green} - 1/\lambda_{red\ edge}) * \lambda_{near\ infrared}$ (Gitelson *et al.* 2001a)

Where λ_{green} is 530-570nm, $\lambda_{red\ edge}$ is 690-710nm, and $\lambda_{near\ infrared}$ is 750-800nm (Gitelson

et al. 2006, Merzlyak *et al.* 2003).

Extrapolation of ground-based anthocyanin indices to satellite systems has been very

limited. One example was completed in the Amazon using a hyperspectral sensor,

NASA's Hyperion, where an anthocyanin index was indicative of drought stress (Asner

et al. 2004). To date, no one has developed a form of anthocyanin detection using more

widely available multispectral satellites such as MERIS, MODIS or Landsat TM/ETM+.

This study aims to test the ability of Hyperion, MERIS, MODIS, and Landsat TM/ETM+

to accurately detect and quantify anthocyanin through simulating satellite bands from

laboratory-based hyperspectral data.

Methods

Medium: Ten sugar maple trees located near Durham, NH were sampled weekly (9/2,

9/9, 9/16, 9/23, 9/30, 10/7, 10/14, 10/21, 10/28) over the fall of 2008, resulting in over

seven hundred leaf samples. The trees were sampled in the morning, from the southern aspect, from the lower two thirds of the outer canopy (van den Berg and Perkins 2007). Samples were collected and stored in a Ziploc bag with a wet paper towel and kept in a cooler with frozen blue ice until measured. Each leaf was measured using a Visible/Infrared Intelligent Spectrometer (VIRIS) (GER 2600[1], Geophysical and Environmental Research Corporation, Millbrook, NY) three times, in progressive 90 degree rotations, for an average reflectance value from each leaf.

Representation of anthocyanin concentrations:

While a combination of wavelengths ($1/R564 - 1/R697$) was found to have a higher correlation with extracted anthocyanin concentrations in sugar maple leaves than other anthocyanin indices (see Chapter 2), this relationship has not been tested on different species. Several studies have found the anthocyanin index created by Gitelson *et al.* (2001a) is able to determine anthocyanin concentrations in a variety of vegetative types (Hoch *et al.* 2003, Merzlyak *et al.* 2003, Steele *et al.* 2008). Due to pixel size and a variable forest composition, a variety of tree species will be viewed by the satellite sensors when actual imagery is used. Therefore, the previously published hyperspectral anthocyanin reflectance indices (hARI) represented in Equations 1 and 2, will be used as a best representation of anthocyanin concentration throughout the present study as it has been tested on a variety of vegetation types (Gitelson *et al.* 2001a). When comparing simulated satellite results based on Equation 2, which has a near infrared component, the hARI will be multiplied by $\lambda_{near\ infrared}$ (Equation 2).

---

[1] The use of specific brand names is for clarity only and does not imply endorsement.

Equations: The different equations used are based on the fact that reflectance at λ_{green} is a combination of chlorophyll reflectance and anthocyanin absorption, whereas reflectance at $\lambda_{red\ edge}$ is only affected by chlorophyll concentration and has been found to be correlated to the reflectance at λ_{green} due to chlorophyll; by subtracting $\lambda_{red\ edge}$ from λ_{green} the result is anthocyanin signature (Equation 1). Two other terms can be introduced, one is a near infrared component which considers the difference in leaf structure (Equation 2), and the other is a log term which is introduced to account for the non-linear relationship between concentration and reflectance (Equation 3) (Buschmann and Nagel 1993, Blackburn 1999). Satellite bands used for these terms can be seen in Table 1.

Equation 3. Concentration based ARI $= (1/\lambda_{green} - 1/\lambda_{red\ edge})^* \log(\lambda_{green})$

Where λ_{green} is 530-570nm and $\lambda_{red\ edge}$ is 690-710nm (Gitelson *et al.* 2006, Merzlyak *et al.* 2003).

Another anthocyanin index has been developed by taking a ratio of the red and green wavelengths (Equation 4). This relationship will also be simulated. Instead of using the summation of several bands for each component, only one red band and one green band were used for the ratio for consistency in comparing different satellites.

Equation 4. Red:Green $= \dfrac{\sum\limits_{i=600}^{699} Ri}{\sum\limits_{i=500}^{599} Ri}$ where R is reflectance (Sims and Gamon 2002).

Satellites:

Hyperion: Hyperion is a hyperspectral sensor which has narrow spectral bands approximately 10nm wide. It has a spatial resolution of 30m². Hyperion imagery must be ordered for acquisition. As a hyperspectral sensor, the bands that match the hARIs (Equations 1 and 2) best are band 20 (543-554nm), 35 (696-707nm), and 40 (747-758nm).

MERIS: MERIS is ESA's MEdium Resolution Imaging Spectrometer but its spectral bands are still narrow, varying between 2.5nm to 10nm. For this study, the reduced resolution product was used which has a spatial resolution of approximately 1200m². Repeat coverage occurs every 3 days. To best match the hyperspectral ARIs (Equations 1 and 2) bands 5 (550-570nm), 9 (700-710nm), and 10 (750-758nm) are used.

MODIS: MODIS is NASA's MOderate Resolution Imaging Spectrometer with spectral bands that range from 20nm to 50nm wide. Its spatial resolution depends on the band and viewing angle, varying from 250m to 1km². Repeat coverage occurs every 1-2 days, but is typically complied into an eight day composite. To best match hyperspectral anthocyanin indices (Equations 1 and 2), bands 1 (620-670nm), 2 (841-876nm), and 4 (545-565nm) were used.

Landsat: Landsat TM/ETM+ is a medium resolution radiometer which has larger spectral bands, averaging together 70nm to 270nm. It has a spatial resolution of 30m². Repeat coverage occurs every 16 days. Landsat's bands are very broad to match the wavelengths in hyperspectral anthocyanin indices (Equations 1 and 2). The best match occurs with bands 2 (520-600nm), 3 (630-690nm), and 4 (760-900nm).

Bands: Satellite bands which were the closest match to the bands used in the hARI were targeted to create simulated satellite anthocyanin indices (Figure 3-1). Simulated bands were created by weighting each hyperspectral band within the range of the satellite band by the relative spectral response of that satellite band. These values were then averaged to produce a value for each simulated band. Table 3-1 shows which satellite bands were used to calculate each satellite ARI.

Table 3-1. Satellite bands which correspond best with the components of the hyperspectral anthocyanin index (hARI).

Satellite	λ_{green}	Band (nm)	$\lambda_{red\ edge}$	Band (nm)	$\lambda_{near\ infrared}$	Band (nm)
Hyperion	Band 20	548.9 ±11	Band 35	701.5 ±10.5	Band 40	752.4 ±10.7
MODIS	Band 4	555 ±10	Band 1	645 ±25	Band 2	876 ±35
MERIS	Band 5	560 ±5	Band 9	705 ±5	Band 10	753.75 ±3.75
Landsat TM/ETM+	Band 2	560 ±40	Band 3	660 ±30	Band 4	830 ±70

Figure 3-1. Satellite band locations in reference to a typical leaf reflectance curve. See Table 3-2 for band information.
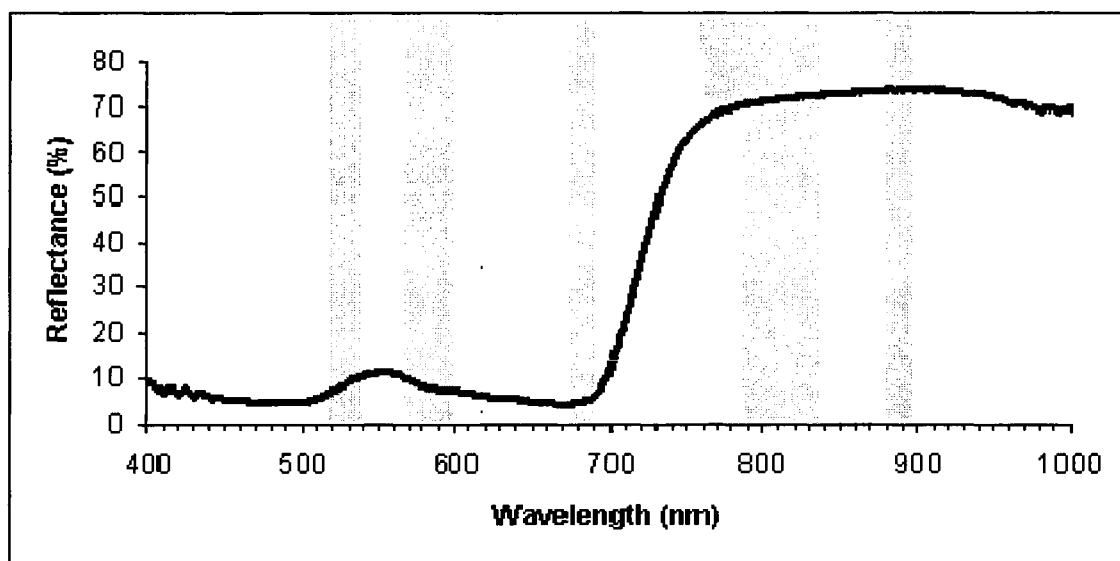
Table 3-2. Satellite band colors and numbers for Figure 1.

Satellite	Color	Bands from left to right
Landsat TM/ETM+	yellow	2, 3, 4
MODIS	red	4, 1, 2
Hyperion	blue	20, 35, 40
MERIS	green	5, 9, 10, 12

Results

Some simulated satellite ARIs (MERIS, MODIS and Landsat TM/ETM+) had difficulty detecting low levels of anthocyanin when coupled with higher chlorophyll levels-- a trait characteristic of leaves sampled in September to early October (Figure 3-2). Due to the number of samples, these early fall leaves dominate the analysis for correlation, but do not show how accurate the indices are after each index's sensitivity increases. Therefore each satellite was analyzed with all points, and secondarily with these early fall leaves excluded.

Figure 3-2. Early fall leaves, indicated by the oval, tend to have higher chlorophyll concentrations and lower anthocyanin concentrations. Concentrations were based on reflectance indices: anthocyanin (1/R550-1/R700) and chlorophyll (RARS) (Chappelle 1992, Gitelson *et al.* 2001a).
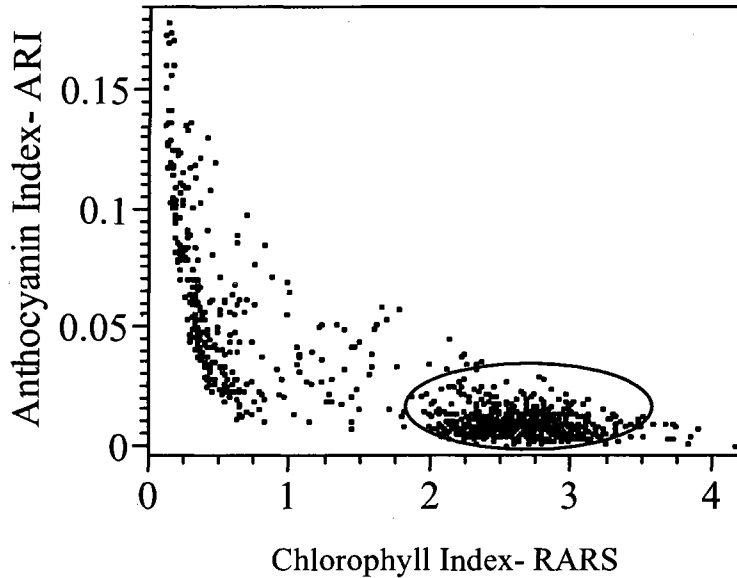
Hyperion: Hyperion's simulated anthocyanin indices performed well in correlation to the hARI (Figure 3). The relationship between the Hyperion ARI and the hARI has a very close fit (r^2= 0.996; Figure 3-3A), showing that the simulated Hyperion satellite should easily detect variations in anthocyanin concentration. Addition of the $\lambda_{near\ infrared}$ term does not result any change, and the fit is still highly correlated (r^2= 0.996; Figure 3-3B). The log decreased fit slightly (r^2= 0.944; Figure 3-3C). Comparing the hARI with the red:green ratio (Equation 3) shows that this index is not the best fit (r^2= 0.932; Figure 3-3D), but it is still an accurate representation of concentration values.

Figure 3-3. Correlation between Hyperion anthocyanin indices and hyperspectral anthocyanin indices. ARIln= concentration based ARI (Equation 3). Correlations to relationships shown can be found in Table 3-3.
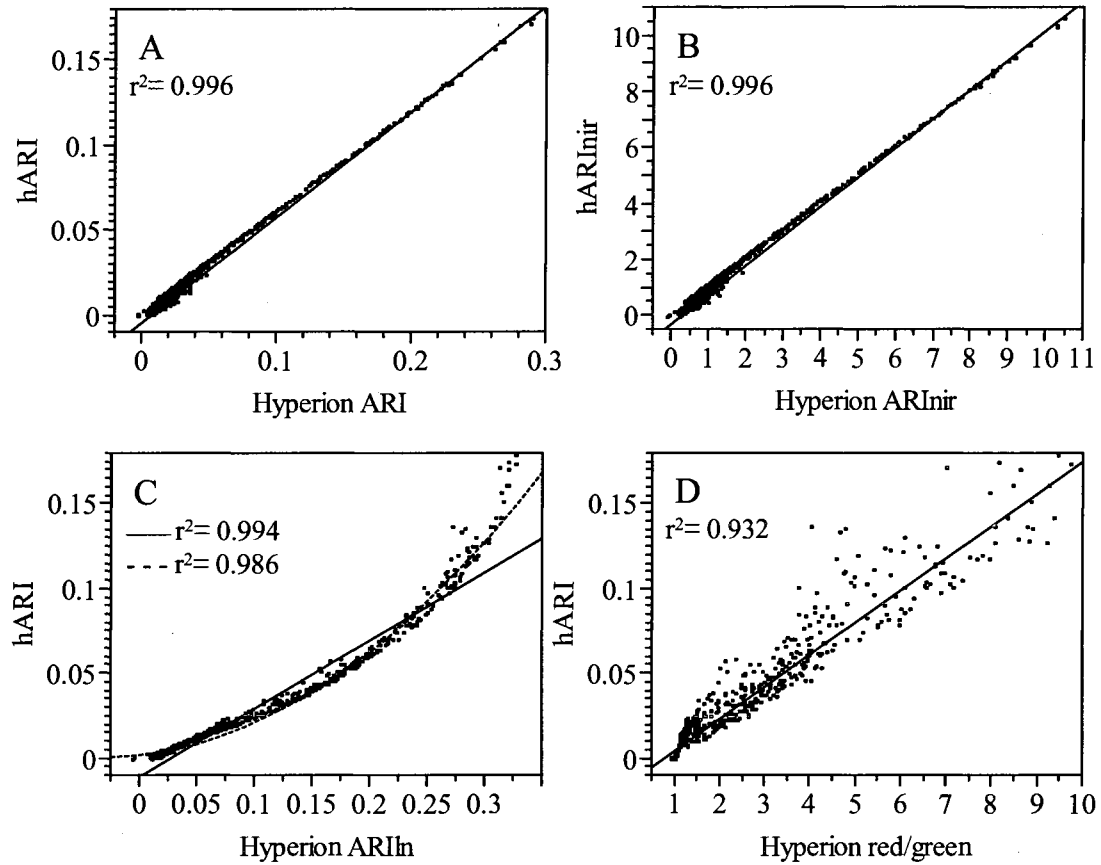
MERIS: MERIS deviates from a linear relationship with hARI (r^2= 0.73; Figure 3-4A). While most late fall leaves follow a linear relationship, the early fall leaves clump together. Detection of anthocyanin in these leaves is being overestimated; for example a leaf with a hARI value of 0.005 has a MERIS ARI value of 0.02-0.07.

Addition of the $\lambda_{near\ infrared}$ term reduces the correlation (r^2=0.691; Figure 3-4B). The log term increases correlation (r^2=0.83; Figure 3-4C). The red:green ratio has the best fit out

of the possible indices (r^2=0.85; Figure 3-4D) and does not experience the problem of early fall leaves separating and causing a non-linear fit.

Table 3-3. Correlation of satellite anthocyanin indices with hyperspectral indices. Landsat ARI's were based on bands available on TM and ETM+. *denotes that value was added to bring index values above 0. Threshold= value below which samples were excluded from analysis. Obs= number of observations.

ALL POINTS	linear r^2	RMSE	non-linear fit	non-linear r^2	RMSE
ARI versus					
Hyperion ARI	0.996	0.002			
MERIS ARI B9	0.73	0.017			
MERIS ARI B8	0.74	0.017	Cubic	0.909	0.01
MODIS ARI*	0.566	0.022	Cubic	0.796	0.015
Landsat ARI*	0.762	0.016	Quadratic	0.914	0.01
ARI nir versus					
Hyperion ARInir	0.996	0.13			
MERIS ARInir B9	0.691	1.094			
MERIS ARInir B8	0.749	0.987	Cubic	0.904	0.61
MODIS ARInir*	0.593	1.257	Cubic	0.828	0.818
Landsat ARInir*	0.76	0.965	Quadratic	0.888	0.661
ARI versus					
Hyperion ARIln	0.944	0.008	Quadratic	0.986	0.004
MERIS ARIln B9	0.826	0.014	Quadratic	0.887	0.011
MERIS ARIln B8	0.685	0.017	Cubic	0.892	0.011
MODIS ARIln	0.6	0.021	Cubic	0.801	0.015
Landsat ARIln	0.759	0.016	Quadratic	0.896	0.011
ARI versus					
Hyperion ARI	0.932	0.009			
MERIS ARI B7: B5	0.838	0.013			
MERIS ARI B9: B5	0.93	0.009			
MERIS ARI B8: B5	0.832	0.014	*not graphed		
MODIS ARI red:green	0.845	0.013			
Landsat ARI red:green	0.854	0.013			

If the early fall leaves can be eliminated from analysis through the use of a threshold value, a better relationship may be possible. It is difficult to apply a threshold as the points are not easily separated based on their MERIS ARI value. If only values above 0.08 of the MERIS ARI are considered the linear fit increases in correlation (Table 3-4). Yet this reduces the number of observations considered to 115 of the possible 890.

Table 3-4. Correlation of satellite anthocyanin indices with hyperspectral indices after threshold values have been used. Landsat ARI's were based on bands available on TM and ETM+. *denotes that value was added to bring index values above 0. Threshold= value below which samples were excluded from analysis. Obs= number of observations.

THRESHOLD	linear r^2	RMSE	non-linear fit	non-linear r^2	RMSE
ARI versus					
Hyperion ARI					
MERIS B9 Obs: Threshold: 0.08	0.791	0.178			
MERIS B8 Obs: Threshold: 0	0.833	0.016			
MODIS ARI Obs: Threshold: -0.01	0.655	0.023			
Landsat ARI Obs: Threshold: 0	0.926	0.01			
ARI nir versus					
Hyperion ARInir					
MERIS ARInir B9	0.962	0.41			
MERIS ARInir B8	0.833	0.921			
MODIS ARInir	0.711	1.201			
Landsat ARInir	0.856	0.839			
ARI versus					
MERIS ARIln B9	0.952	0.008	Quadratic	0.978	0.005
MERIS ARIln B8	0.739	0.0197	Quadratic	0.865	0.0142
MODIS ARIln	0.604	0.024			
Landsat ARIln	0.899	0.12	Square root	0.93	0.01

The simulated MERIS data takes a similar form to MODIS and Landsat TM/ETM+ when Band 8 (677.5-685nm) is used as it is closer to the red wavelengths (Figure 3-5). While Band 9 allows for the closest linear fit, there are complications with anthocyanin being over estimated. Band 8 separates the data more, as the early fall leaves clump together in the negative values of the index and are underestimated versus overestimated. If zero were to be used as a threshold the number of observations considered increases to 262 and the linear prediction is more accurate (r^2= 0.833). While Band 8 performs better in the ARI's based on subtraction, Band 9 performs better in the red:green ratio (Table 3-

3). Using the near infrared Band 9 in the red:green ratio performs better than using Band

7 (660-670nm) which is a closer representation of reflectance in the red (Table 3-3).

Figure 3-4. Correlation between MERIS anthocyanin indices using band 9 and hyperspectral anthocyanin indices. ARIln= concentration based ARI (Equation 3). Correlations to relationships shown can be found in Table 3-3.
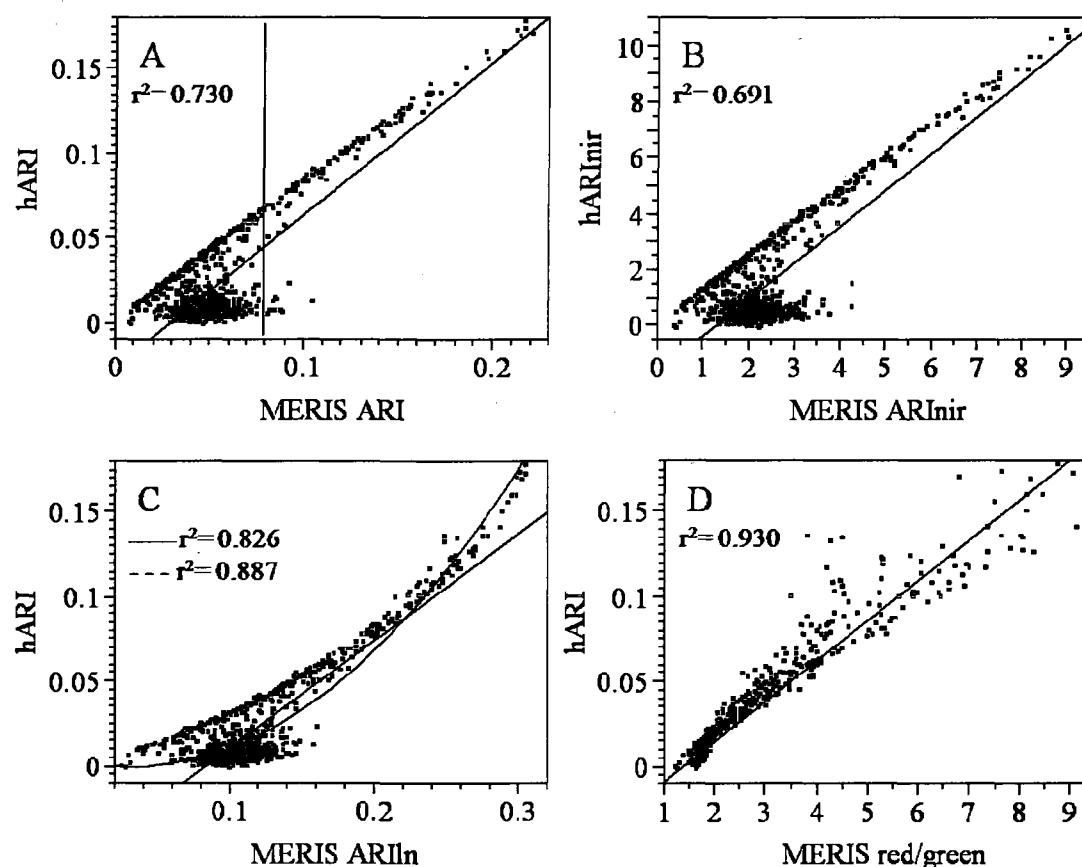
Figure 3-5. Correlation between MERIS anthocyanin indices using band 8 and hyperspectral anthocyanin indices. ARIln= concentration based ARI (Equation 3). Correlations to relationships shown can be found in Table 3-3.
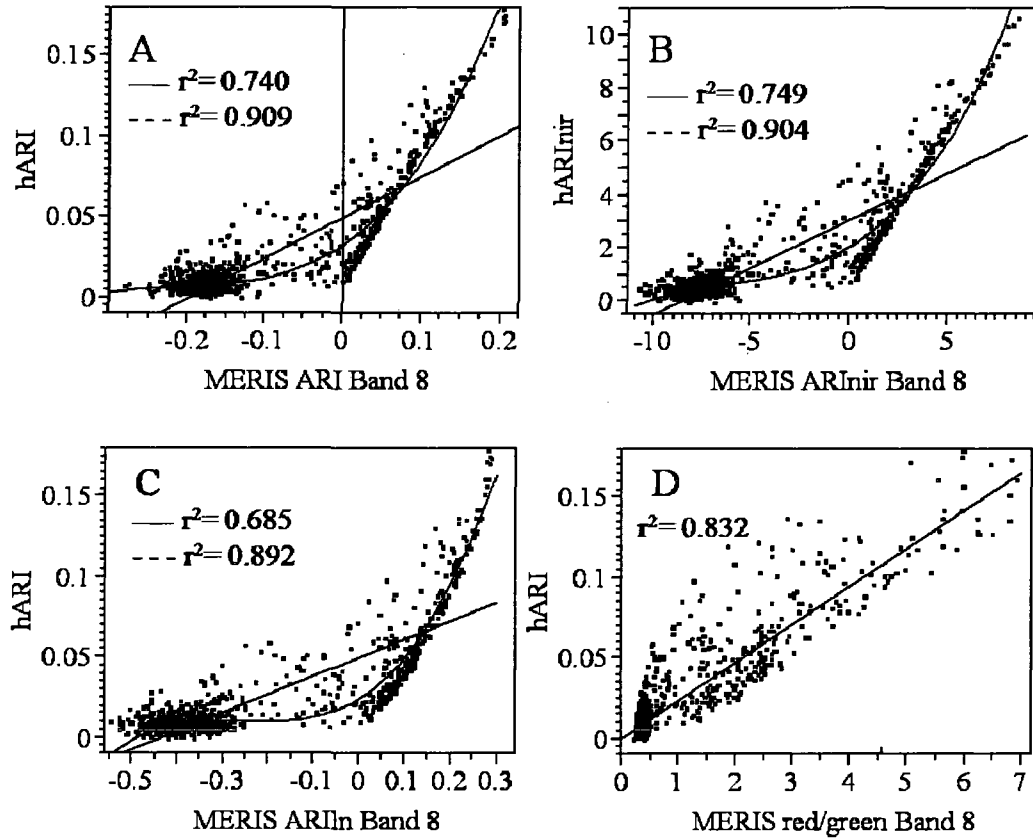
MODIS: The MODIS ARI is not highly linearly correlated with the hARI ($r^2 = 0.566$; Figure 3-5A). Using a cubic function increases the correlation to hARI ($r^2 = 0.796$). The cubic function fits better because the index values of MODIS are split into two sets (Figure 3-5A). The lower values of the MODIS ARI match early fall leaves. The addition of the $\lambda_{near\ infrared}$ component increases the fit slightly when compared to a linear relationship ($r^2 = 0.59$; Figure 3-5B). The $\lambda_{near\ infrared}$ component also increases the correlation when using a cubic fit ($r^2 = 0.828$; Figure 3-5B) compared to the non-linear hARI fit. Using the log term may be useful here due to the broader spectral bands and

increases the linear fit (r^2= 0.60; Figure 3-5C). It also slightly increases the fit using a

cubic relationship (r2= 0.80; Figure 3-5C). Since the early fall leaves deviate from a

linear relationship, a threshold value may be useful to increase the correlation, albeit

while reducing the power of the index. By excluding MODIS ARI values lower than

-0.01, the analysis is based on 305 observations. The correlation to hARI increases

slightly (r^2= 0.60). The addition of the $\lambda_{near\ infrared}$ term increases the correlation (r^2=

0.71), and the addition of the log term decreases fit (r^2= 0.60).

The best fit out of all these relationships when considering all observations occurs with

the red:green ratio (r^2= 0.85).

Figure 3-6. Correlation between MODIS anthocyanin indices and hyperspectral
anthocyanin indices. ARIln= concentration based ARI (Equation 3). Correlations to
relationships shown can be found in Table 3-3.
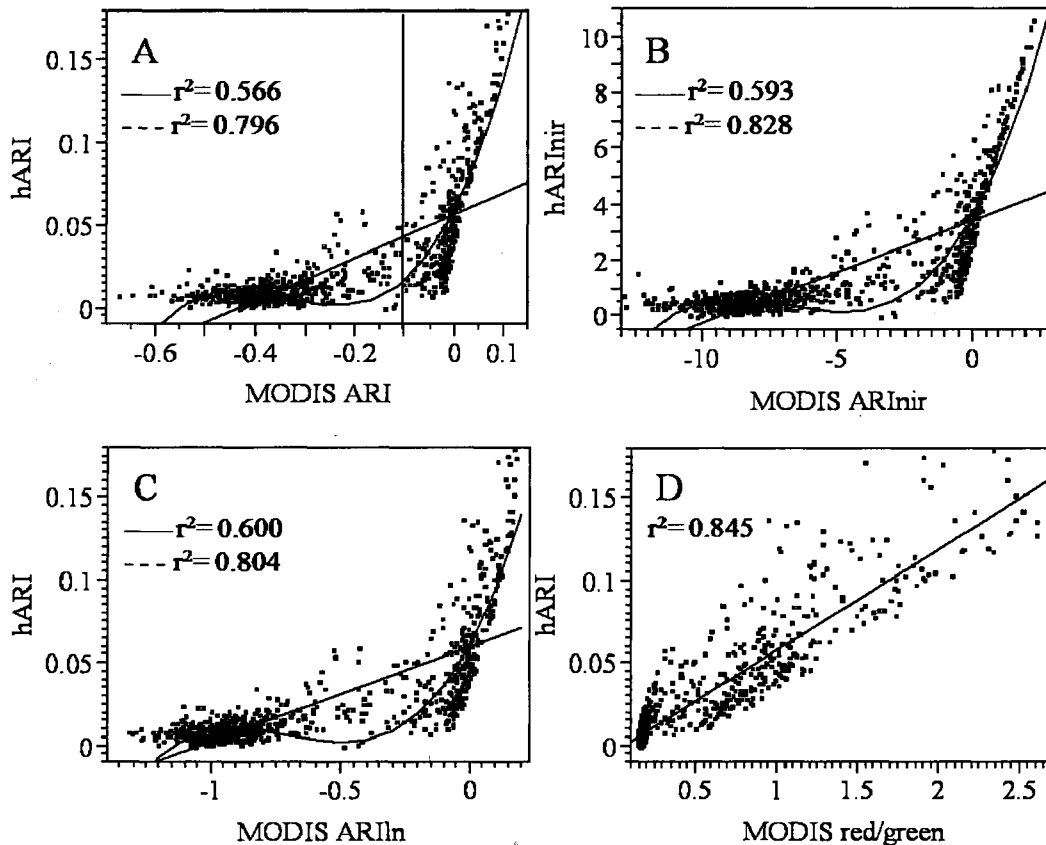
Landsat: The simulated Landsat ARI TM/ETM+ is modestly correlated to a linear fit of the hARI (r^2= 0.76). This performance of this relationship increases greatly when considering a non-linear fit (quadratic, r^2= 0.91). The addition of the $\lambda_{near\ infrared}$ term or the log term decreases fit in both the linear and non-linear relationships (Table 3-3). The Landsat TM/ETM+ ARI shows two groups of observations which accounts for why a linear relationship is not the best fit (Figure 3-6). These two groups are either early or late fall observations. Since detection of the early fall leaves proves problematic, a threshold can be applied. If values below 0 are excluded, the fit of the Landsat TM/ETM+ ARI to the hARI increases (r^2= 0.93) although the power of the index has decreased. If the log or $\lambda_{near\ infrared}$ terms are added the fit decreases slightly (Table 3-4).

The red:green ratio performs well when considering all samples (r^2=0.85). Although there is some scatter with this index, the early fall leaves don't assume a non-linear relationship.

Figure 3-6. Correlation between Landsat TM/ETM+ anthocyanin indices and hyperspectral anthocyanin indices. ARIln= concentration based ARI (Equation 3). Correlations to relationships shown can be found in Table 3-3.
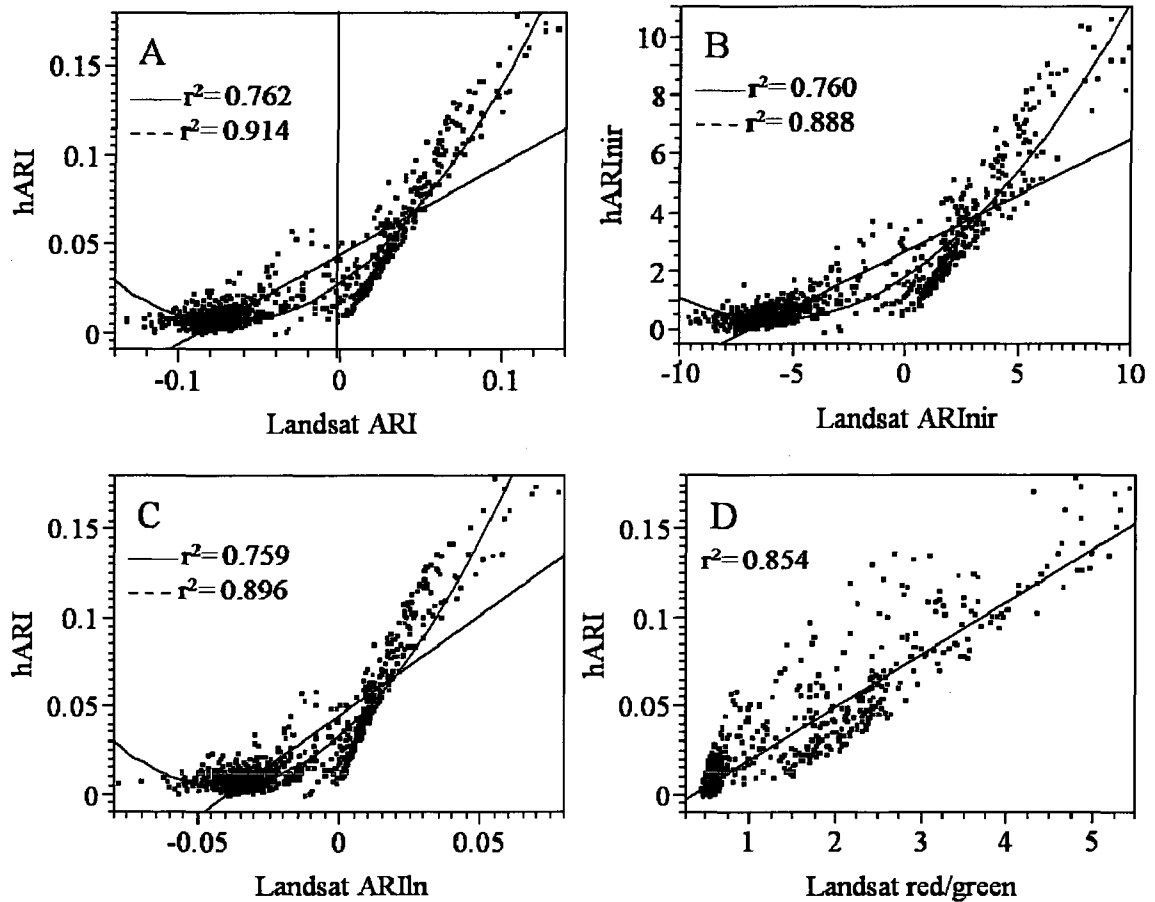

Discussion

For all multispectral satellites the best approximation came from using the red:green ratio with the exception of Landsat TM/ETM+. The red:green ratio works well for Landsat TM/ETM+ (r^2= 0.854), but a better fit can be obtained using a non-linear fit to any of the ARI approximations—including those with log and $\lambda_{near\ infrared}$ terms.

There are two modifications that can be made to the basic ARI. One is the addition of the near infrared band to account for difference in structure in leaves. For all modeled

satellites, this did not improve the fit except for the linear fit of MODIS; the linear fit of MODIS is not a very good approximation of the relationship between the hARI and satellite ARI and therefore should not be considered. The insignificance of the near infrared component in this study may be due to the use of a homogeneous single species of maple; this may change when real imagery is considered and a more heterogeneous scene with mixed forest stands within a single pixel is considered.

The second modification that can be made is to add the log of reflectance at 550nm. This accounts for the non-linear relationship between pigment reflectance and concentration. The addition of this term did not increase correlation between the hARI and the simulated satellite ARI's for Hyperion or Landsat TM/ETM+ (Figures 3-3C and 3-6C). The correlation increased for MODIS and MERIS slightly when compared to linear fits (Figures 3-4C and 3-5C). When a non-linear fit for the MODIS log ARI is used, the correlation increases ($r^2 = 0.89$). If a non-linear relationship is used for the MODIS log ARI, the correlation increases slightly over the non-linear fit to the MODIS ARI (Table 3-3). Overall, addition of the log term does not seem to improve fit significantly.

Threshold values were used to increase the correlation between satellite ARI's and the hARI, but make the indices less powerful as values below the threshold can not be interpreted. It is difficult to determine a threshold value for MERIS as green leaves are consistently over estimated using Band 9. Unlike MODIS and Landsat TM/ETM+ where high chlorophyll/low anthocyanin leaves are underestimated and there is a value difference between the early fall leaves and late fall leaves, the MERIS data are more

clumped causing the threshold to exclude more data. After low anthocyanin/high chlorophyll leaves are excluded, the MERIS ARI follows a linear relationship. Leaves detected after this exclusion may still have a green appearance, but in general correspond to leaves that are further senesced and chlorophyll degradation is apparent. When using Band 8 for MERIS, the relationship to the hARI looks similar to Landsat TM/ETM+ and MODIS. Here, a threshold value excludes less data than the MERIS Band 9 threshold and predicts the hARI with more certainty. It may be that Band 9 falls too far up the red edge, causing less reciprocal reflectance, representing chlorophyll, to be subtracted. While early anthocyanin detection might be difficult, it may be that MERIS will perform well because the tops of canopies change first during fall senescence; this might send a falsely high signal back to the satellite and anthocyanin may be detected before "peak color" occurs throughout the canopy. Yet in terms of tourism, many people view foliage at overlooks where only the tops of the trees can be seen and therefore MERIS could provide an adequate representation of the landscape.

Landsat TM/ETM+ also performed well after an obvious threshold was used and its application may be easier than MERIS. The Landsat TM/ETM+ threshold excluded fewer samples indicating that although the index may not be as precise as MERIS, it may be able to detect anthocyanin development earlier. It is also important to note that although Landsat TM/ETM+ data have some advantages (30m pixels, long historic record), the 16 day repeat cycle limits it's usefulness in comparing annual peak color characteristics.

Even after high chlorophyll leaves were excluded, MODIS correlation to the hARI did not improve as significantly as MERIS or Landsat TM/ETM+. This may be due to the higher amount of scatter MODIS experienced versus the other satellites which comes from a wider spread of values for the early fall leaves in the negative values of the MODIS index. The fact that the MODIS band 15 falls short of the wavelengths used in the hARI for the near infrared region may explain its lack of fit. The MODIS $\lambda_{red\ edge}$ is not the best proxy to equal the amount of reflectance due to chlorophyll at 550nm as the reflectance values in the sensor's range are typically lower than those at the more ideal 700nm, and therefore the index will subtract more reflectance from the 550nm component (as the relationship is inversed).

Conclusions

Overall, the red:green ratio correlated best with multispectral satellite ARI's and the hARI. Non-linear relationships with some satellites also performed well, but indicate a change in the relationship between satellite bands and the hyperspectral bands as ideally results would show a linear relationship. Hyperion gave the best fit when compared with the other satellite systems (MERIS, MODIS and Landsat TM/ETM+) included in this study. This was a theoretical exercise to test which satellites should be focused on for further study of remote sensing to detect fall foliage.

CHAPTER 4

APPLYING ANTHOCYANIN INDICES TO HYPERSPECTRAL AND
MULTISPECTRAL IMAGING

Abstract

Remote detection of plant pigments has given great insight into ecosystem function.

While some pigment indices have been developed for satellite systems, there is not yet

one for anthocyanin. Anthocyanin, a red pigment, is a general indicator of plant stress;

satellite detection of this pigment could enhance understanding of different plant

processes and how plants respond to a changing environment. Laboratory-based

hyperspectral anthocyanin indices were extrapolated to several multispectral satellite

platforms. Detection of a seasonal signal known to develop in New England in the fall

was targeted to see if satellites could acquire reliable data for detecting changes in

anthocyanin concentrations. Hyperion, MERIS, and MODIS were able to detect a

seasonal signal using two different indices to represent anthocyanin concentrations.

Further study is needed to find the accuracy and sensitivity of these indices in practice.

Introduction

Anthocyanin is a red pigment found in many plant species and can be seen throughout New England during the autumn. Anthocyanin is thought to be a universal indicator of plant stress formed in response to a number of conditions including photoinhibition, oxidative and osmotic stress, nutrient deficiency, and wounding (Chalker-Scott 1999, Close and Beadle 2003, Gould 2004). Detecting its presence would therefore be useful for ecosystem analysis and for monitoring changes during autumn senescence.

Climate change will affect fall foliage by changing the conditions which contribute to anthocyanin synthesis. Increased temperatures in the fall are associated with muted foliage colors (NECIA 2006, NERA 2007). The predicted increase of drought in the summer and fall will possibly decrease leaf color expression (NECIA 2006). Sugar maples are also in danger of disappearing as a dominant species type as their habitat shifts –as shown by both the low emissions and high emissions scenarios examined by the US Global Change Research Program (Barron 2001, Iverson and Prasad 2001). Plant pigments react to environmental stresses, such as those induced by climate change. It may be possible to track stress to sugar maples, and other species, if a satellite-based anthocyanin index is developed.

Satellite detection of anthocyanin could provide useful insight into a number of different ecosystems. For instance, anthocyanin is associated with gradual and delayed chlorophyll accumulation during leaf expansion of many rainforest plants (Close and Beadle 2003). Nutrient deficiency, which affects photosynthetic productivity, is also

associated with anthocyanin production and therefore could be a useful diagnostic tool (Atkinson 1973, Bhandal and Malik 1988, Hodges and Nozzolillo 1996, Kumar and Sharma 1999, Trull *et al.* 1997). Anthocyanin develops in many crop plants; for instance in cotton, increasing anthocyanin concentrations are correlated with crop maturity and could be used as a management tool (Phillips 2006).

As sugar maple trees senesce throughout the fall, anthocyanin develops. This color change attracts millions of visitors every year (Development 2007). Anthocyanin development comes to a height, called peak color, then leaves continue to degrade and eventually fall off. Detection of this color wave could be useful to the tourism industry as well as increase our understanding on why this phenomenon occurs.

The most accurate way to measure pigment concentrations is through destructive analysis. Research has explored the development of non-destructive assessment methods through the use of remote sensing. Absorption and reflectance features have been characterized for anthocyanin and hyperspectral indices have been created to eliminate influence of other pigments (Merzylak *et al.* 1999, Gitelson and Merzylak 2004). These hyperspectral indices used for anthocyanin quantification typically use a two or three band ratio. A band, λ_{green}, accounts for anthocyanin absorbance and chlorophyll reflectance, while the band $\lambda_{red\ edge}$ estimates chlorophyll's reflectance in the λ_{green} region. By subtracting the $\lambda_{red\ edge}$ from λ_{green} the result is an anthocyanin signature; some indices also include a band in the near infrared to account for leaf structure (Merzylak *et al.* 1999, Gitelson *et al.* 2001a, Sims and Gamon 2002, Gitelson *et al.* 2006).

Extrapolation of ground-based anthocyanin indices to satellite systems has been very limited. One example was conducted in the Amazon with a hyperspectral sensor, Hyperion, where an anthocyanin index was thought to be indicative of drought stress (Asner *et al.* 2004). To date, no one has developed a form of anthocyanin detection using more widely available multispectral satellites such as MERIS, MODIS and Landsat TM/ETM+. Extrapolation of hyperspectral indices to multispectral satellites was simulated and a correlation was found between these simulated satellite responses and anthocyanin concentration (Chapter 3).

This paper aims to apply anthocyanin indices to data acquired by Hyperion, MERIS, and MODIS sensor systems to see if a fall seasonal signal can be detected. This is a theoretical study to see which satellites should be considered for future study. No ground truthing occurred for any satellite and minimal satellite processing was employed since this part of the study was for developing a "proof-of-concept" example.

Methods

Equations: The different equations used are based on the fact that reflectance at λ_{green} is a combination of chlorophyll reflectance and anthocyanin absorption, whereas reflectance at $\lambda_{red\ edge}$ is only affected by chlorophyll concentration and has been found to be correlated to the reflectance at λ_{green} due to chlorophyll; by subtracting $\lambda_{red\ edge}$ from λ_{green} the result is an anthocyanin signature (Equation 1). Another term which can be introduced is a near infrared component which considers the difference in leaf structure (Equation 2).

Equation 1. hARI= $1/\lambda_{green}$ - $1/\lambda_{red\ edge}$ (Gitelson *et al.* 2001a)

Equation 2. $hARI_{nir}$= $(1/\lambda_{green}$ - $1/\lambda_{red\ edge})$* $\lambda_{near\ infrared}$ (Gitelson *et al.* 2001a)

Where λ_{green} is 530-570nm and $\lambda_{red\ edge}$ is 690-710nm and "h" denotes that it is a

hyperspectral index (Gitelson *et al.* 2006, Merzlyak *et al.* 2003).

Another anthocyanin index was developed by Sims and Gamon (2002) by taking a ratio

of the red and green wavelengths (Equation 3). This hyperspectral index has been found

to work in a single species study of coastal live oak, but was not found to be correlated to

anthocyanin concentrations in a study with mixed species. This relationship will also be

tested in this study. Instead of using the summation of several bands for each component

as done for hyperspectral sensors, only one red band and one green band were used for

the ratio of each satellite, including Hyperion. This was done for consistency in order to

compare satellites with different spectral resolutions.

$$\text{Equation 3. Red:Green} = \frac{\sum_{i=600}^{699} Ri}{\sum_{i=500}^{599} Ri} \quad \text{(Sims and Gamon 2002).}$$

<u>Bands:</u> Satellite bands which were the closest match to the bands used in the hARI were

used to create the satellite anthocyanin indices (Equation 1). Figure 4-1 shows the

placement of all satellite bands used for these indices. Table 4-1 shows which satellite

bands were used to calculate each satellite ARI.

Table 4-1. Satellite bands used to create each satellite anthocyanin index.

Satellite	λ_{green}	Band (nm)	$\lambda_{red\ edge}$	Band (nm)	$\lambda_{near\ infrared}$	Band (nm)
Hyperion	Band 20	548.9 ±11	Band 35	701.5 ±10.5	Band 40	752.4 ±10.7
MODIS	Band 4	555 ±10	Band 1	645 ±25	Band 2	876 ±35
MERIS	Band 5	560 ±5	Band 9	705 ±5	Band 10	753.75 ±3.75
Landsat TM/ETM+	Band 2	560 ±40	Band 3	660 ±30	Band 4	830 ±70

Figure 4-1. Satellite band locations in reference to a typical leaf reflectance curve. See Table 2 for band information.

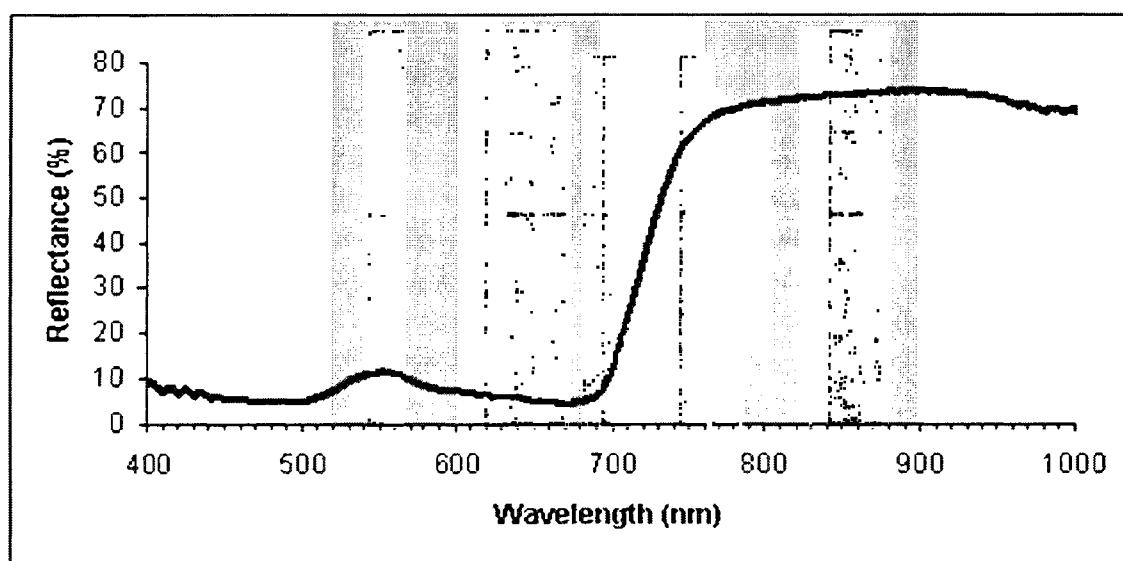Table 4-2. Satellite band colors and numbers for Figure 1.

Satellite	Color	Bands from left to right
Landsat TM/ETM+	yellow	2, 3, 4
MODIS	red	4, 1, 2
Hyperion	blue	20, 35, 40
MERIS	green	5, 8, 9, 10, 12

Satellites:

Hyperion: Hyperion is a hyperspectral sensor which has small spectral bands approximately 10nm wide. It has a spatial resolution of $30m^2$. Two Hyperion images— September 17, 2008 and October 10, 2008-- were obtained for analysis (EO-1 Hyperion satellite images provided by NASA- National Aeronautics and Space Agency). The level one product was converted to surface reflectance using ACORN v.5 (Imspec LLC). No geo-rectification was made and target areas were matched between the two scenes by eye using prominent geographic features. As a hyperspectral sensor, the best bands which match the ARI are band 20 (543-554nm), 35 (696-707nm), and 40 (747-758nm).

MERIS: MERIS is a MEdium Resolution Imaging Spectrometer but its spectral bands are still narrow, ranging between 2.5nm to 10nm. For this study, the reduced resolution product was used which has a spatial resolution of approximately $1200m^2$. Repeat coverage occurs every 3 days. MERIS imagery from 9/19, 10/11, 10/17, 10/20, and 10/23/2008 were obtained (Envisat MERIS satellite images provided by ESA- European Space Agency). The preprocessed surface reflectance product was used. No geo-rectification occurred and target areas between scenes were matched by eye using prominent geographic features. To best match the hyperspectral ARI bands 5 (550-570nm), 9 (700-710nm), and 10 (750-758nm) are used. Band 8 (677.5-685nm) was also used as an approximation of $\lambda_{red\ edge}$.

MODIS: MODIS is a MOderate Resolution Imaging Spectrometer with spectral bands that range from 20nm to 50nm wide. Its spatial resolution is approximately $1km^2$. Repeat coverage occurs every 1-2 day, but data is typically complied into an 8-day composite. Surface reflectance products for MODIS were downloaded from Oak Ridge

National Lab (ORNL) for 9/13, 9/21, 9/29, 10/7, 10/15, and 10/23/2008 (ORNL 2009).

These images were already geo-corrected and latitude/longitude coordinates were used to

match locations between scenes. After investigation of the data, 9/29/2008, was flagged

as suspicious and excluded from analysis. For emulating the hyperspectral anthocyanin

index, bands 1 (620-670nm), 2 (841-876nm), and 4 (545-565nm) we used.

Seasonal analysis: Fall foliage changes in the higher elevations and higher latitudes first,

and then progresses south and to lower elevations (Vermont Vacation 2009). Over the

course of the fall anthocyanin development increases, reaches a peak concentration

(hereafter referred to as peak color), and then declines (Figure 4-2). The seasonal

progression of anthocyanin development, peak, and decline should be evident in the plot

of satellite ARI's over time.

Figure 4-2. An example of anthocyanin development throughout the fall. Data obtained
from field samples taken in Durham, NH.
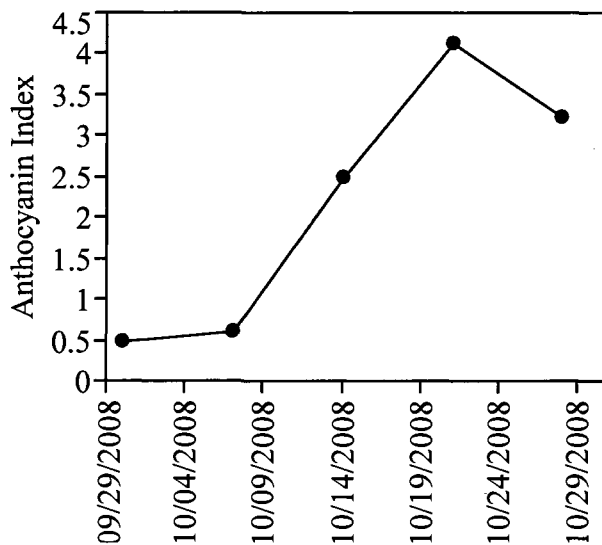
Locations: Two locations were targeted for analysis (Figure 4-3). The Mount

Washington valley was targeted as the northern location which experiences color change

starting in late September to early October. Loudon, New Hampshire was targeted as a

southern location which experiences color change in mid- October. Loudon was the

closest location seen by all satellites to the field site used for determining anthocyanin

indices (see Chapter 2 and 3).

Figure 4-3. Location of sites targeted for imagery analysis, the Mt. Washington valley and Loudon, as well as the field site location (Durham, NH).
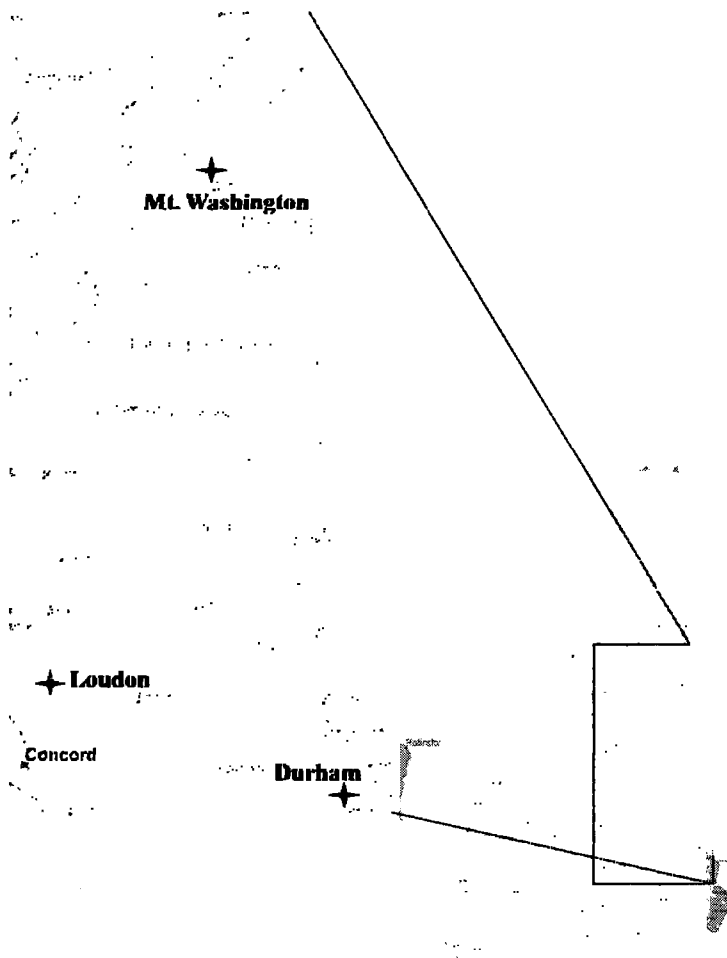
Results and Discussion

<u>Hyperion:</u>

Hyperion was used as a gauge to determine if anthocyanin detection by satellites is possible since its bands most closely match that of the hyperspectral anthocyanin indices. Two images, one early foliage season and another mid-season were compared. A visual difference in the amount of red can be seen with the eye (Figure 4-4, panels A and C). ARI images were made for both dates (Figure 4-4, panels B and D) where black indicates less anthocyanin and white indicates more anthocyanin. Both ARI images have the same data scaling so the overall lightening between the two images represents an overall increase in anthocyanin between these two dates. There are a few geographic features in these images which are inconsistent in the amount of anthocyanin detected; this may be due to the effect of shadowing or due to the elevation profile. Overall, areas that look more red in the 10/10 image than the 9/17 image are a lighter color in the 10/10 ARI image than the 9/17 ARI image.

Another anthocyanin index, the red:green ratio (Equation 3), is shown in panel E for 10/10/2008 (Figure 4-4). The red:green image is very similar to the ARI image for this date, but may not be as sensitive to small changes as the image shows less value differences than the ARI image. Although a sensitivity analysis can not be performed, Hyperion seems capable of detecting changes in anthocyanin concentrations.

Figure 4-4. These are true color Hyperion images (bands 30, 20, 10) from the same geographic location for 9/17/08 (A) and 10/10/09 (C). B is the ARI for 9/17/08 and D is the ARI for 10/10/09. E is a red:green ratio for 10/10/09. Darker color indicates little to no anthocyanin, while lighter colors correspond to anthocyanin development.

A   B   C   D   E
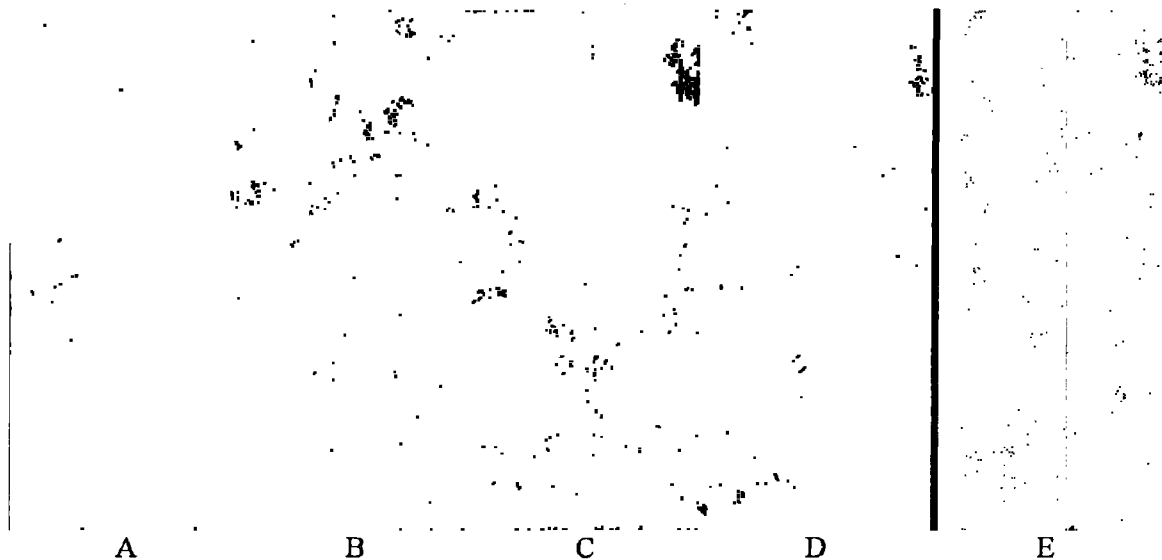
MODIS:

While exclusion of the 9/19 date due to quality issues leaves a gap, neither location

should experience a peak in color by this date. If this date was available it would have

allowed for better consideration of the rate of anthocyanin development. As it is shown,

the timing of anthocyanin development at the Loudon site seems early, but no

conclusions can be drawn from this due to the lack of data from 9/19. Using Equation 2,

a MODIS composite was constructed over the course of the fall (Figure 4-5). Initial

development is evident in both locations. It is also evident that the northern location,

Mount Washington, starts accumulating anthocyanin sooner than Loudon. The signal for

Loudon seems to follow the correct seasonal trend. Due to its southern location, Loudon

should experience anthocyanin decay although this may be more evident after another

week. The Mount Washington signal does not have a clear peak. One would expect

more decay on the 10/23 date versus an increase, but overall the seasonal signal is present. Leaving out the $\lambda_{near\ linfrared}$ component (Equation 1) did not improve the seasonal signal and showed similar results to the MODIS ARI_{nir}.

Using the red:green ratio to represent anthocyanin concentrations results in a more realistic seasonal signal for Mount Washington. This representation also preserved the correct relationship between the north and southern sites, with initial development and an earlier peak of anthocyanin occurring in the north. While the Loudon signal shows continuing anthocyanin development instead of a peak, as one would expect, the rate of development has slowed.

Figure 4-5. MODIS ARI_{nir} plotted over time for both Mount Washington and Loudon locations.
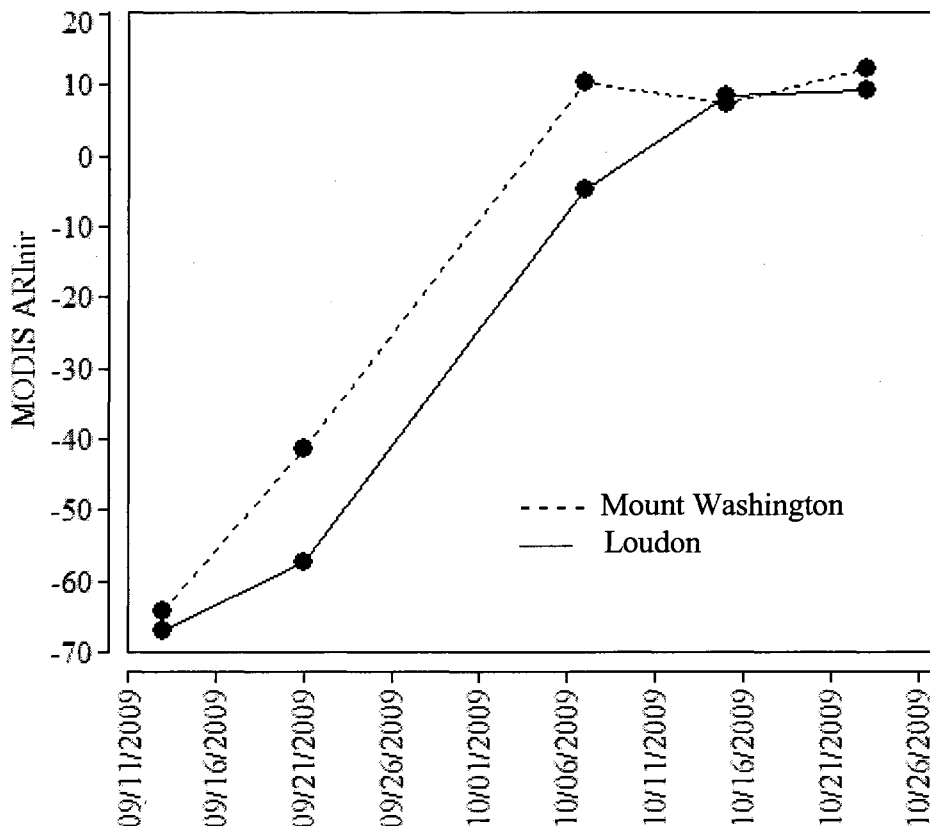
Figure 4-6. MODIS red:green ratio over time for both the Mount Washington and Loudon locations.
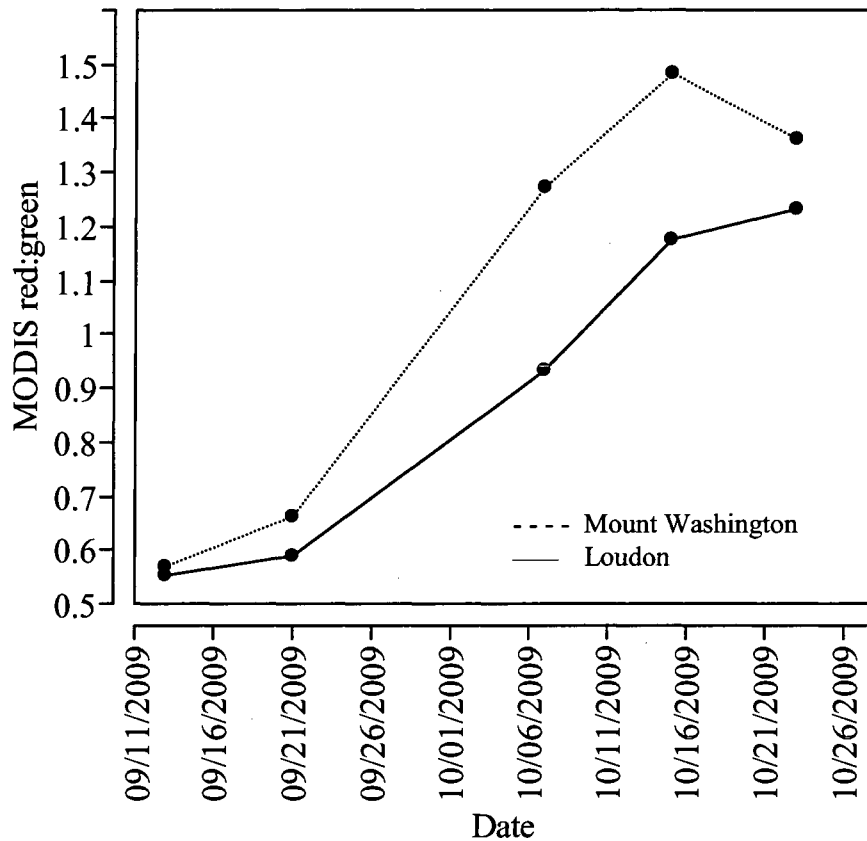
MERIS:

The MERIS ARI$_{nir}$ which most closely matches the wavelengths specified in the hyperspectral ARI does not perform well (Figure 4-7). It shows a continuous decline throughout the fall. The lack of detection using Band 9 is surprising as MERIS has the closest match of $\lambda_{red\ edge}$ to the hARI out of all the multispectral satellites. It may be that band 9 is too far up the red edge where reflectances are higher, therefore subtracting less due to the use of reciprocals in the ARI equation (Equation 1). If this is true, $\lambda_{red\ edge}$ would be small, leaving the MERIS's satellite ARI using band 9 based mainly on $1/\lambda_{green}$.

It may be that using band 9 results in a signal more dominated by chlorophyll than anthocyanin.

Using band 8 (677.5-685nm) results in a better representation of the seasonal foliage signal (Figure x). This ARI index shows initial development and peak color earlier in the north than the south, which follows general foliage trends. Band 8 would therefore be more useful in anthocyanin estimation than band 9 when using Equations 1 and 2.

Using the red:green ratio for MERIS (bands 5 and 6) shows a similar signal as the MERIS ARI_{nir} using band 8. The initial changes in the north are seen before the south, which follows the known progression of fall foliage. The red:green ratio shows a more exaggerated change after the peak. Without ground validation it is not possible to know which seasonal signal is more accurate.

Overall either MERIS index, ARI_{nir} based on band 8 or the red:green ratio can detect changes in anthocyanin concentrations.

Figure 4-7. MERIS ARI_{nir} plotted over time for both the Mount Washington and Loudon locations. Panel A shows the MERIS ARI_{nir} based on Band 9 for $\lambda_{red\ edge}$ whereas panel B shows the MERIS ARI_{nir} based on Band 8 for $\lambda_{red\ edge}$.
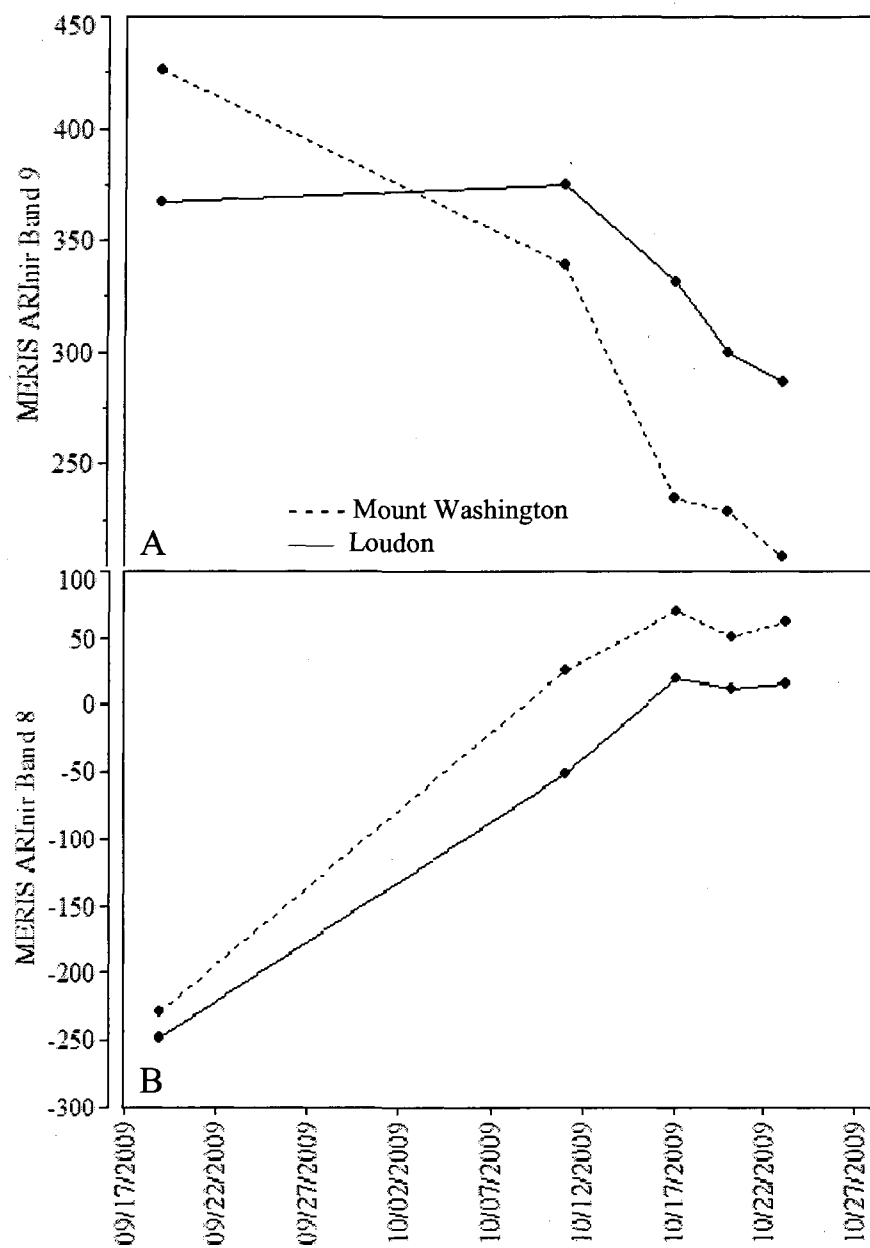
Figure 4-8. MERIS red:green ratio over time for both Mount Washington and Loudon locations using bands 6 and 5.
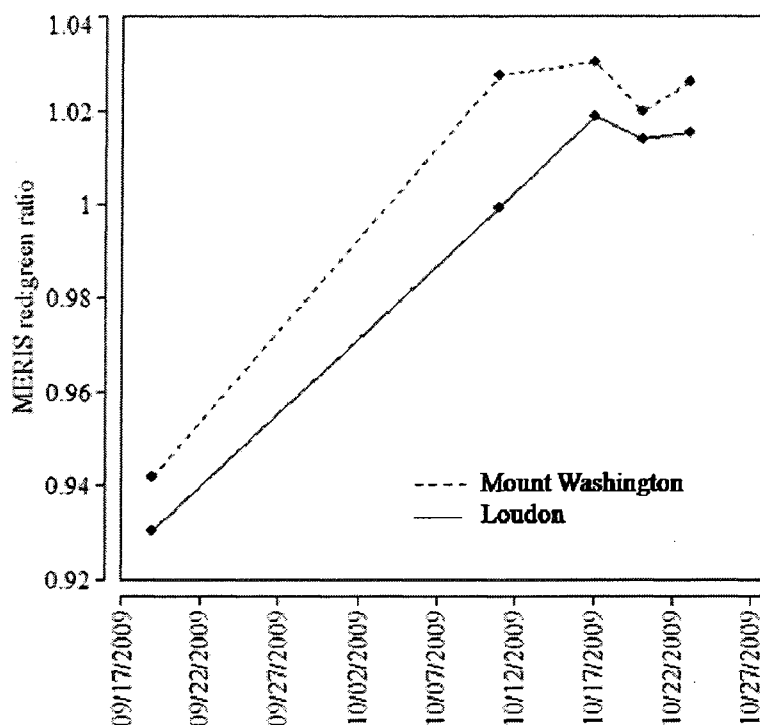
Landsat TM/ETM+:

While simulated Landsat TM/ETM+ based ARI's performed well in predicting

anthocyanin concentrations (Chapter 3), its lengthy 16-day repeat coverage makes it

difficult to use. Anthocyanin concentrations change quickly and getting imagery every

two weeks, possibly with cloud cover, is not a fine enough temporal resolution for this

application.

Conclusions

Hyperion, MERIS, and MODIS all show some capacity to detect anthocyanin changes over the course of the fall. Overall, using red:green ratios for any satellite seems to produce a reliable seasonal signal. Using anthocyanin indices based on Equations 1 and 2 also produce reasonable seasonal signals (when using Band 8 for MERIS). Further investigation is needed to compare these signals to ground data in order to determine which most closely represent anthocyanin concentrations and to determine the sensitivities of these indices.

Developing these satellite indices would be helpful in order to understand the phenomenon of fall foliage. Currently most quantification of color change, both timing and intensity, is subjective and based on personal experiences. Objective quantification of anthocyanin through satellites would allow scientists to use archival data and assess changes in the character of fall foliage over the past few decades. While Landsat was not useful in the present study, developing an anthocyanin index to be used in its long term archives could apply to other research. Beyond fall foliage, anthocyanin development may be useful for characterizing stress in different ecosystems or be applied to climate change studies, particularly in phenology.

LIST OF REFERENCES

70

Aber, J. and J. Melillo (2001). *Terrestrial Ecosystems*. Academic Press: San Diego. 556p.

Adamsen, F. J., P. J. Pinter Jr. and E. M. Barnes (1999). Measuring wheat senescence with a digital camera. *Crop Science* 39: 719-724.

Agati, G., S. Meyer, P. Matteini and Z. Cerovic (2007). Assessment of anthocyanins in grape (*Vitis vinifera* L.) berries using a noninvasive chlorophyll fluorescence method. *Journal of Agricultural and Food Chemistry* 55: 1052-1061.

Anderson, O. and K. Markham, Eds. (2006). Flavonoids : chemistry, biochemistry, and applications. CRC, Taylor and Francis: Boca Raton, FL. 1237p.

Asner, G. P., D. Nepstad, G. Cardinot and D. Ray (2004). From The Cover: Drought stress and carbon uptake in an Amazon forest measured with spaceborne imaging spectroscopy. *Proceedings of the National Academy of Sciences* 101(16): 6039-6044.

Asrar, G., M. Fuchs, E. Kanemasu and J. Hatfield (1984). Estimating absorbed photosynthetic radiation and leaf area index from spectral reflectance in wheat. *Agronomy Journal* 76: 300-306.

Atkinson, D. (1973). Some general effects of phosphorous deficiency on growth and development. *New Phytologist* 72: 101-111.

Bardon, R. (2007). "Changing Color." Retrieved 3/24/2008 from http://www.ces.ncsu.edu/.

Barron, E. (2001). Potential consequences of climate variability and change for the northeastern United States. *Climate Change Impacts on the United States*. U. G. C. R. Program eds. 109-134.

Beggs, C. and E. Wellmann (1985). Analysis of light controlled anthocyanin formation in coleoptiles of *Zea mays* L.: The role of UV-B, blue, red, and far-red light. *Photochemistry and Photobiology* 41: 481-486.

Bhandal, D. and C. Malik (1988). Potassium estimation, uptake and its role in the physiology and metabolism of flowering plants. *International Review of Cytology* 110: 205-254.

Blackburn, G. (1998). Quantifying chlorophylls and carotenoids at leaf and canopy scales: an evaluation of some hyperspectral approaches. *Remote Sensing of Environment* 66: 273-285.

Blackburn, G.A (1999) Relationships between spectral reflectance and pigment concentrations in stacks of deciduous broadleaves. *Remote Sensing of Environment* 70:224-237.

Blackburn, G. (2007). Hyperspectral remote sensing of plant pigments. *Journal of Experimental Botany* 58: 855-867.

Bowler, C., G. Neuhaus, H. Yamagata and N. Chua (1994). Cyclic GMP and calcium mediated phytochrome phototransduction. *Cell* 77: 73-81.

Brandt, K., A. Giannini and B. Lercari (1995). Photomorphologenic responses to UV radiation, III: A comparative study of UV-B effects on anthocyanin and flavonoid accumulation in wild-type and *aurea* mutant of tomato. *Photochemistry and Photobiology* 62: 1081-1087.

Burger, J. and G. Edwards (1996). Photosynthetic efficiency, and photodamage by UV and visible radiation, in red versus green leaf Coleus varieties. *Plant and Cell Physiology* 37: 395-399.

Buschmann C. and E. Nagel (1993). In vivo spectroscopy and internal optics of leaves as basis for remote sensing of vegetation. *International Journal of Remote Sensing* 14: 711-722.

Caldwell, M., R. Robberecht and S. Flint (1983). Internal filters: Prospects for UV-acclimation in higher plants. *Physiologia Plantarum* 58: 445-450.

Carter, G. (1994). Ratios of leaf reflectances in narrow wavebands as indicators of plant stress. *International Journal of Remote Sensing* 15: 697-703.

Chalker-Scott, L. (1999). Environmental significance of anthocyanins in plant stress responses. *Photochemistry and Photobiology* 70: 1-9.

Chaney, W. (2005). Fantasy, Facts and Fall Color. Purdue University. 5p.

Chang, K., G. Fechner and H. Schroeder (1989). Anthocyanins in autumn leaves of quaking aspen in Colorado. *Forest Science* 35: 229-236.

Chappelle, E., M. Kim and J. McMurtrey (1992). Ration analysis of reflectance spectra (RARS): an algorithm for the remote estimation of the concentrations of chlorophyll a, chlorophyll b, and carotenoids in soybean leaves. *Remote Sensing of Environment* 39: 239-247.

Christie, P., M. Alfenito and V. Walbot (1994). Impact of low-temperature stress on general phenylpropanoid and anthocyanin pathways: Enhancement of transcript abundance and anthocyanin pigmentation in maize seedlings. *Planta* 194: 541-549.

Clatterbuck, W. (1999). Changing color of leaves. The University of Tennessee Agricultural Extension Service. 4p.

Close, D. and C. Beadle (2003). The ecophysiology of foliar anthocyanin. *The Botanical Review* 69: 149-161.

Coder, K. (2007). Autumn Leaf Colors. Warnell School of Forestry & Natural Resources, University of Georgia: Athens, GA. 7p.

Coley, P. and T. Aide (1989). Red coloration of tropical young leaves: A possible antifungal defense? *Journal of Tropical Ecology* 5: 293-300.

Cottam, W. (1966). Quaking Aspen. *Proceedings of the 42nd International Shade Tree Conference*: 243-254.

Curran, P., J. Dugan, B. Macler and S. Plummer (1991). The effect of a red leaf pigment on the relationship between red edge and chlorophyll concentration. *Remote Sensing of Environment* 35: 69-76.

Dale, V. H., L. A. Joyce, S. McNulty, R. P. Neilson, M. P. Ayres, M. D. Flannigan, P. J. Hanson, L. C. Irland, A. E. Lugo, C. J. Peterson, D. Simberloff, F. J. Swanson, B. J. Stocks and B. M. Wotton (2001). Climate change and forest disturbances. *BioScience* 41(9): 723-734.

Datt, B. (1998). Remote sensing of chlorophyll *a*, chlorophyll *b*, chlorophyll *a+b*, and total carotenoid content in Eucalyptus leaves. *Remote Sensing of Environment* 66: 111-121.

Decendit, A. and J. Mérillon (1996). Condensed tannin and anthocyanin production in *Vitis vinifera* cell suspension cultures. *Plant Cell Reports* 15: 762-765.

Development, N. D. o. T. a. T. (2007). "Fall Foliage New England." Retrieved 2/5, 2007, from http://www.visitnh.gov/fall-foliage-new-england.html.

Ehlenfeldt M.K. and R.L. Prior (2001). Oxygen radial absorbance capacity (ORAC) and phenolic anthocyanin concentrations in fruit and leaf tissues of highbush blueberry. *Journal of Agricultural and Food Chemistry* 49:2222-2227.

Feild, T., D. Lee and N. Holbrook (2001). Why leaves turn red in autumn. The role of anthocyanins in senescing leaves of red-osier dogwood. *Plant Physiology* 127: 566-574.

Fukshansky, L., A. Remiowsky, J. McClendon, A. Ritterbusch, T. Ricther and H. Mohr (1993). Absorption spectra of leaves corrected for scattering and distributional error : a radiative transfer and absorption statistics treatment. *Photochemistry and Photobiology* 57: 538-555.

Gamon, J. and J. Surfus (1999). Assessing leaf pigment content and activity with a reflectometer. *New Phytologist* 143: 105-117.

Gitelson, A. and M. Merzlyak (1994). Spectral reflectance changes associate with autumn senescence of *Aesculus hippocastanum* L. and *Acer platanoides* L. leaves: spectral features and relation to chlorophyll estimation. *Journal of Plant Physiology* 143: 286-292.

Gitelson, A. A., M. N. Merzlyak and O. B. Chivkunova (2001a). Optical properties and nondestructive estimation of anthocyanin content in plant leaves. *Photochemistry and Photobiology* 74(1): 38-45.

Gitelson, A., M. Merzlyak, Y. Zur, R. Stark and U. Gritz (2001b). Non-destructive and remote sensing techniques for estimation of vegetation status. Proceedings of the 3rd European Conference on Precision Agriculture 1. p.205-210.

Gitelson, A. and M. Merzlyak (2004). Non-destructive assessment of chlorophyll, carotenoid and anthocyanin content in higher plant leaves: principles and algorithms. *Remote Sensing for Agriculture and the Environment*. S. Stamatiadis, J. M. Lynch and J. S. Schepers eds. Ella, Greece. p.78-94.

Gitelson, A., G. Keydan and M. Merzlyak (2006). Three-band model for noninvasive estimation of chlorophyll, carotenoids, and anthocyanin contents in higher plant leaves. *Geophysical Research Letters* 33: L11402.

Goodwin, T. (1958). Studies in carotenogenesis. XXIII. The changes in carotenoid and chlorophyll pigments in the leaves of deciduous trees during autumn necrosis. *Biochemical Journal* 68: 503-511.

Gould, K (2004). Nature's swiss army knife: the diverse protective roles of anthocyanin in leaves. *Journal of Biomedicine and Biotechnology* 5: 314-320.

Gould, K. and B. Quinn (1999). Do anthocyanins protect leaves of New Zealand native species from UV-B? *New Zealand Journal of Botany* 37: 175-178.

Hamilton, W. and S. Brown (2001). Autumn tree colours as a handicap signal. *Proceedings of the Royal Society of London B* 268: 1489-1493.

Harborne, J. B. (1967). *Comparative biochemistry of the flavonoids*. Academic Press: New York. 383p.

Harvard Forest (2009). "The science of leaf color change." Retreived 7/2, 2008. from harvardforest.fas.harvard.edu/research/leaves/science.html.

Himelblau, E. and R. Amasino (2001). Nutrients mobilized from leaves of *Arabidopsis thaliana* during leaf senescence. *Journal of Plant Physiology* 158: 1317-1323.

Hoch, W., E. Singaas and B. McCown (2003). Resorption protection. Anthocyanins facilitate nutrient recovery in autumn by shielding leaves from potentially damaging light levels. *Plant Physiology* 133:1296-1305.

Hodges, D. and C. Nozzolillo (1996). Anthocyanin and anthocyanoplast content of cruciferous seedlings subjected to mineral nutrient deficiencies. *Journal of Plant Physiology* 147: 749-754.

Hörtensteiner, S. and U. Feller (2002). Nitrogen metabolism and remobilization during senescence. *Journal of Experimental Botany* 53: 927-937.

Huete, A. R. (1988). A soil-adjusted vegetation index (SAVI). *Remote Sensing of Environment* 25: 295– 309.

Hussey, G. (1963). Growth and development in young tomato. II. The effect of defoliation on the development of the shoot apex. *Journal of Experimental Botany* 14: 326-333.

Inouye, D. (2000). The ecological and evolutionary significance of frost in the context of climate change. *Ecology Letters* 3: 457-463.

IPCC (2007). *Climate Change 2007 The Physical Science Basis*. Cambridge University Press: New York. 989p.

Ishikura, N. (1973). The changes in anthocyanin and chlorophyll content during the autumnal reddening of leaves. *Kumamoto Journal of Science* 11: 43-50.

Isman, M. and S. Duffey (1982). Toxicity of tomato phenolic compounds to the fruitworm, *Helopthis zea. Entomologia experimentalis et applicata* 31: 370-376.

Iverson, L. and A. Prasad (2001). Potential changes in tree species richness and forest community types following climate change. *Ecosystems* 4:186-199.

Janzen, D. (1979). New horizons in the biology of plant defenses. *Herbivores: their interactions with secondary plant metabolites*. G. Rosenthal, D. Janzen and S. Applebaum eds. Academic Press: New York. p. 331-350.

Jeannette, E., A. Reyss, N. Grégory, P. Gantet and J.-L. Prioul (2000). Carbohydrate metabolism in a heat-girdled maize source leaf. *Plant, Cell & Environment* 23: 61-69.

Ji, S., M. Yokoi, N. Saito and L. Mao (1992). Distribution of anthocyanins in *Aceraceae* leaves. *Biochemical Systematics and Ecology* 20: 771-781.

Keskitalo, J., G. Bergquist, P. Gardestrom and S. Jansson (2005). A cellular timetable of autumn senescence. *Plant Physiology* 139: 1635-1648.

Kim, M., C. Daughtry, E. Chappelle, J. McMurtrey III and C. Walthall (1994). The use of high spectral resolution bands for estimating absorbed photosynthetically active radiation (Apar). *Proceedings of the 6th Symposium on Physical Measurements and Signatures in Remote Sensing* Val D'Isere, France, January 17–21, 299–306.

Knox, G. (1989). Water use and average growth index of five species of container grown woody landscape plants. *Journal of Environmental Horticulture* 7: 136-139.

Kozlowski, T. and S. Pallardy (1997). *Physiology of Woody Plants*. Academic Press: San Diego. 411p.

Kramer, P. (1979). *Physiology of Woody Plants*. Academic Press: New York. 824p.

Krol, M., G. Gray, V. Hurry, G. Oquist, L. Malek and N. Huner (1995). Low temperature stress and photoperiod affect an increased tolerance to photoinhibition in *Pinus banksiana* seedlings. *Canadian Journal of Botany* 73: 119-1127.

Kumar, V. and S. Sharma (1999). Nutrient deficiency-dependent anthocyanin development in *Spirodela polyrhiza* L. Schleid. *Biologica Plantarum* 42: 621-624.

Landry, L., C. Chapple and R. Last (1995). *Arabidopsis* mutants lacking phenolic sunscreens exhibit enhanced ultraviolet-B injury and oxidative damage. *Plant Physiology* 109: 1159-1166.

Larronde, F., S. Krisa, A. Decendit, C. Chéze, G. Deffieux and J. Mérillon (1998). Regulation of polyphenol production on *Vitis vinifera* cell suspension cultures by sugars. *Plant Cell Reports* 17: 946-950.

Lee, D. (1987). The spectral distribution of radiation in two neotropical rainforests. *Biotropica* 19: 161-166.

Lee, D., J. O'Keefe, N. Holbrook and T. Feild (2003). Pigment dynamics and autumn leaf senescence in a New England deciduous forest, eastern USA. *Ecological Research* 18: 677-694.

Leng, P., H. Itamura, H. Yamamura and X. Deng (2000). Anthocyanin accumulation in apple and peach shoots during cold acclimation. *Scientia Horticulturae* 83: 43-50.

Lichtenthaler, H. (1987). Chlorophyll fluorescence signatures of leaves during autumnal chlorophyll breakdown. *Journal of Plant Physiology* 131: 101-110.

Mancinelli, A. (1983). The photoregulation of anthocyanin synthesis. *Photomorphogenesis*. W. Shropshire and H. Mohr eds. Springer-Verlag: Berlin. p. 640-661.

Markham, K., K. Ryan, K. Gould and G. Richards (2000). Cell wall sited flavonoids in *Lisianthus* flower petals. *Phytochemistry* 54: 681-687.

McClure, J. (1975). Physiology and functions of flavonoids. *The Flavonoids*. J. B. Harborne, T. Mabry and H. Mabry eds. Academic Press: New York. 1204 p.

Menzel, A. and P. Fabian (1999). Growing season extended in Europe. *Nature* 397: 659.

Merzlyak, M., A. Gitelson, S. Pogosyan, O. B. Chivkunova, L. Lehimena, M. Garson, N. Buzulukova, V. Shevyreva and V. Rumyantseva (1997). Reflectance spectra of leaves and fruits during their development and senescence and under stress. *Russian Journal of Plant Physiology* 44: 707-716.

Merzlyak, M., A. Gitelson, O. B. Chivkunova and V. Y. Rakitin (1999). Non-destructive optical detection of pigment changes during leaf senescence and fruit ripening. *Physiologia Plantarum* 106: 135-141.

Merzlyak, M. and O. B. Chivkunova (2000). Light-stress-induced pigment changes and evidence for anthocyanin photoprotection in apples. *Journal of Photochemistry and Photobiology B: Biology* 55: 155-163.

Merzlyak, M., A. Gitelson, O. B. Chivkunova, A. Solovchenko and S. Pogosyan (2003). Application of reflectance spectroscopy for analysis of higher plant pigments. *Russian Journal of Plant Physiology* 50: 785-792.

Merzlyak, M., A.E. Solovchenko and A. Gitelson (2003). Reflectance spectral features and non-destructive estimation of chlorophyll, carotenoid and anthocyanin content in apple fruit. *Postharvest Biology and Technology* 27: 197-211.

Minocha, R., G. Martinez, B. Lyons and S (2009). Long. Development of a standardized methodology for quantifying total chlorophyll and carotenoids from foliage of hardwood and conifer tree species. *Canadian Journal of Forest Research* 39: 849-861.

Murakami, P., F. Paula, M. Turner, A. van den Berg and P. Schaberg (2005). An instructional guide for leaf color analysis using digital imaging software. U. S. Service, 33p.

Murray, J., A. Smith and W. Hackett (1994). Differential dihydroflavonol reductase transcription and anthocyanin pigmentation in the juvenile and mature phases of ivy (*Hedera helix* L.). *Planta* 194: 102-109.

Myers, V.I. (1970). Soil, Water, and Plant Relations. Remote Sensing with Special Reference to Agriculture and Forestry. National Research Council. National Academy of Sciences: Washington D.C. 424p.

Nakayama, T. and J. Powers (1972). Absorption spectra of anthocyanin *in vivo*. *The chemistry of plant pigments*. C. Chichester eds. New York: Academic Press. 218p.

NECIA (2006). Climate Change in the U.S. Northeast: A report of the Northeast Climate Impacts Assessment (NECIA). Union of Concerned Scientists. 52p.

Neill, S. and K. Gould (1999). Optical properties of leaves in relation to anthocyanin concentration and distribution. *Canadian Journal of Botany* 77: 1777-1782.

Neill, S., K. Gould, P. Kilmartin, K. Mitchell and K. Markham (2002). Antioxidant capacities of green and cyanic leaves in the sun species, *Quintinia serrata*. *Functional Plant Biology* 29: 1437-1443.

New England Regional Assessment Group (2001). Preparing for a changing climate: the potential consequences of climate variability and change. New England Regional Overview. US Global Change Research Program. University of New Hampshire. 96p.

Norby, R., J. Hartz- Rubin and M. Verbrugge (2003). Phenological responses in maple to experimental atmospheric warming and CO2 enrichment. *Global Change Biology* 9: 1792-1801.

Nozzolillo, C., P. Isabelle and G. Daas (1990). Seasonal changes in the phenolic constituents of jack pine seedlings (*Pinus banksiana*) in relation to the purpling phenomenon. *Canadian Journal of Botany* 68: 2010-2017.

ORNL (2009). Oak Ridge National Laboratory Distributed Active Archive Center (ORNL DAAC). MODIS subsetted land products, collection 5. Accessed 5/19/2009. Available online daac.ornl.gov/MODIS/modis.html from ORNL DAAC Oak Ridge, TN, USA.

Overton, E. (1899). Experiments on the autumn colouring of plants. *Nature* 59: 296.

Paine, T., C. Hanlon, D. Pittenger, D. Ferrin and M. Malinosky (1992). Consequences of water and nitrogen management on growth and aesthetic quality of drought-tolerant woody landscape species. *Journal of Environmental Horticulture* 10: 94-99.

Phillips, T (2006). Spectral Reflectance imagery and baseline analysis of anthocyanin concentration in *Gossypium Hirsutum* L. Masters Thesis, Louisiana State University.

Quiros, C., M. Stevens, C. Rick and M. Kok-Yokomi (1977). Resistance in tomato to the pink form of the potato aphid (*Macrosiphum euphorbiae* Thomas): The role of anatomy, epidermis hairs, and foliage composition. *Journal of the American Society for Horticultural Science* 102: 166-171.

Rabinowitch, E. (1945). *Photosynthesis and related processes*. Interscience Publishers: New York. 599p.

Ribereau-Gayon, P. (1972). *Plant Phenolics*. Hafner Publishing Co.: New York. 254p.

Richardson, A. D., J. P. Jenkins, B. Braswell, D. Hollinger, S. V. Ollinger and M. L. Smith (2007). Use of digital webcam images to track spring green-up in a deciduous broadleaf forest. *Ecosystem Ecology* 152: 323-334.

Rock, B.N., J.E. Vogelmann, D.L. Williams, A.F. Vogelmann and T. Hoshizaki (1986). Remote detection of forest damage. *BioScience* 36: 439-445.

Rock, B. N., T. Hoshizaki and J. R. Miller (1988). Comparison of in situ and airborne spectral measurements of the blue shift associated with forest decline. *Remote Sensing of Environment* 24: 109-127.

Rock, B. N., D. L. Williams, D. M. Moss, G. N. Lauten and M. Kim (1994). High-spectral resolution field and laboratory optical reflectance measurements of red spruce and eastern hemlock needles and branches. *Remote Sensing of Environment* 47: 176-189.

Rosenzweig, C., A. Iglesias, X. Yang, P. Epstein and E. Chivian (2001). Climate change and extreme weather events. *Global Change and Human Health* 2: 90-104.

Schaberg, P., A. van den Berg, P. Murakami, J. Shane and J. Donnelly (2003). Factors influencing red expression in autumn foliage of sugar maple trees. *Tree Physiology* 23: 325-333.

Schmitzer, V., G. Osterc, R.Veberic and F. Stampar (2009). Correlation between chromaticity values and major anthocyanins in seven Acer *palmatum* Thunb. Cultivars. *Scientia Horticulturae* 119: 442-446.

Schrevens, E. and L. Raeymaeckers (1992). Colour characterization of golden delicious apples using digital image processing. *Acta Horticulturae* 304: 159-166.

Sherwin, H. and J. Farrant (1998). Protection mechanisms against excess light in the resurrection plants *Craterostigma wilmsii* and *Xerophyta viscosa*. *Plant Growth Regulation* 24: 203-210.

Shirley, B. W. (1996). Flavonoid synthesis: 'new functions' for an 'old pathway.' *Trends in Plant Science* 1: 301-317.

Sims, D. and J. Gamon (2002). Relationships between leaf pigment content and spectral reflectance across a wide range of species, leaf structures and developmental stages. *Remote Sensing of Environment* 81: 337-354.

Soukupová, J., B.N. Rock and J. Albrechtová (2002). Spectral characteristics of lignin and soluble phenolics in the near infrared- a comparative study. *International Journal of Remote Sensing* 23: 3039-3055.

Smith, M. L., M. E. Martin, L. Plourde and S. V. Ollinger (2003). Analysis of hyperspectral data for estimation of temperate forest canopy nitrogen concentration: Comparison between an airborne (AVIRIS) and a spaceborne (Hyperion) sensor. *IEEE Transaction on Geoscience and Remote Sensing* 41: 1332-1337.

Stapleton, A. and V. Walbot (1994). Flavonoids can protect maize DNA from the induction of ultraviolet radiation damage. *Plant Physiology* 105: 881-889.

Strack D. and V. Wray (1989). Anthocyanins in <u>Methods in Plant Biochemistry</u>Volume <u>1.</u> J.B. Harborne and P.M. Dey eds. Academic Press: New York p. 325-356.

Steele, M., A. Gitelson, D. Rundquist and M. Merzlyak (2008). Nondestructive Estimation of Anthocyanin Content in Grapevine Leaves. *American Journal of Enology and Viticulture* 60: 87-92.

Steponkus, P. and F. Lanphear (1969). The relationship of anthocyanin content to cold hardiness of *Hedera helix*. *Hortscience* 4: 55-56.

Stintzing, F., A. Stintzing, R. Carle, B. Frei and R. Wrolstad (2002). Color and antioxidant properties of cyanidin-based anthocyanin pigments. *Journal of Agricultural and Food Chemistry* 50: 6172-6181.

Swain, T (1965). Nature and Properties of Flavonoids. Chemistry and biochemistry of plant pigments. T.W. Goodwin eds. Academic Press: London. 583p.

Takahaski, A., K. Takeda and T. Ohnishi (1991). Light-induced anthocyanin reduces the extent of damage to DNA in UV-irratiated *Centaurea cyanus* cells in culture. *Plant and Cell Physiology* 32: 541-547.

Teramura, A. (1983). Effects of ultraviolet-B radiation on the growth and yield of crop plants. *Photosynthesis Research* 39: 463-473.

Tourism, New Hampshire Department of Travel and Tourism. (2007). "New Hampshire Division of Travel and Tourism Visitor Barometer." Retrieved 4/11, 2008, from oz.plymouth.edu/inhs/Barometers/3_NH_Travel_Barometer_Fall_2006.doc.

Trull, M. C., M. J. Guiltinan, J. P. Lynch and J. Deikman (1997). The responses of wild-type and ABA mutant *Arabidopsis thaliana* plants to phosphorus starvation. *Plant, Cell & Environment* 20: 85-92.

Tsuda, T., K. Shiga, K. Ohshima, S. Kawakishi and T. Osawa (1996). Inhibition of lipid peroxidation and the active oxygen radical scavenging effect of anthocyanin pigments isolated from *Phaseolus vulgaris* L. *Biochemical Pharmacology* 52: 1033-1039.

Ustin, S. L., M. O. Smith and J. B. Adams (1993). Remote sensing of ecological processes: A strategy for developing and testing ecological models using spectral mixture analysis. *Scaling Physiological Processes: Leaf to Globe.* J. R. Ehelringer and C. B. Field eds. Academic Press: San Diego. p.339-357.

Ustin, S. L., D. A. Roberts, J. A. Gamon, G. Asner and R. O. Green (2004). Using imaging spectroscopy to study ecosystem processes and properties. *BioScience* 54: 523-534.

van den Berg, A. and T. Perkins (2007). Contribution of anthocyanins to the antioxidant capacity of juvenile and senescing sugar maple (*Acer saccharum*) leaves. *Functional Plant Biology* 34: 714-719.

Vermont Vacation (2009). "The Foliage Forecaster." Retrieved 7/16, 2008, from www.vermontvacation.com/seasons/forecaster.asp.

Vogelmann, J. E., B. N. Rock and D. M. Moss (1993). Red edge spectral measurements from sugar maple leaves. *International Journal of Remote Sensing* 14: 1563-1575.

Walther, G. R., E. Post, P. Convey, A. Menzel, C. Parmesan, T. J. Beebee, J. M. Fromentin, O. Hoegh-Guldberg and F. Bairlein (2002). Ecological responses to recent climate change. *Nature* 416: 389-395.

Wang, H., G. Ca and R. Prior (1997). Oxygen radical absorbing capacity of anthocyanins. *Journal of Agricultural and Food Chemistry* 45: 304-309.

Wheldale, M. (1916). *The anthocyanin pigments of plants*. University Press: Cambridge. 318p.

Zakhleniuk, O., C. Raines and J. Lloyd (2001). pho3: a phosphorus- deficient mutant of *Arabidopsis thaliana* (L.) Heynh. *Planta* 212: 529-534.